

## Bulletin of Volcanology

### A proximal record of caldera-forming eruptions: the stratigraphy, eruptive history, and collapse of the Palaeogene Arran caldera, western Scotland

--Manuscript Draft--

<b>Manuscript Number:</b>	BUVO-D-18-00013R2	
<b>Full Title:</b>	A proximal record of caldera-forming eruptions: the stratigraphy, eruptive history, and collapse of the Palaeogene Arran caldera, western Scotland	
<b>Article Type:</b>	Research Article	
<b>Corresponding Author:</b>	Robert James Gooday Cardiff University UNITED KINGDOM	
<b>Corresponding Author Secondary Information:</b>		
<b>Order of Authors:</b>	Robert James Gooday David J Brown Kathryn M Goodenough Andrew C Kerr	
<b>Funding Information:</b>	Natural Environment Research Council (NE/L002434/1)	Mr Robert James Gooday
<b>Abstract:</b>	<p>Caldera-forming volcanic eruptions are among the most dangerous, and can generate extensive pyroclastic deposits and deliver ash into global atmospheric circulation systems. As calderas collapse, the eruptions can deposit thick proximal ignimbrite sequences and thinner ignimbrites more distally. However, the proximal record of caldera collapse is often obscured by later intrusions, volcanism, faults, alteration, water and sediments, which significantly limits our understanding of these eruptions. A Palaeogene caldera system in central Arran, western Scotland, preserves a rare proximal caldera-fill succession, the Arran Volcanic Formation. This caldera largely comprises highly heterogeneous ignimbrites and minor intra-caldera sedimentary rocks. The current level of erosion, and the general absence of faults, intrusions and sediments, allows a complex stratigraphy and collapse history to be determined, which can be linked to changing eruptive styles at a constantly-evolving volcano.</p> <p>The first recorded phase was eruption of a homogeneous rhyolitic lava-like tuff, deposited from high temperature, high mass-flux pyroclastic density currents generated from low fountaining columns that retained heat. A succeeding phase of highly explosive Plinian eruptions, marked by a thick blanket of massive lapilli tuffs, was then followed by piston-like caldera collapse and erosion of steep caldera walls. Volcanism then became generally less explosive, with predominantly lava-like and eutaxitic tuffs and cognate-spatter-rich agglomerates interbedded with non-homogenous lapilli tuffs. High topographic relief between distinct units indicate long periods of volcanic quiescence, during which erosive processes dominated. These periods are, in several places, marked by sedimentary rocks and evidence for surface water, which includes a localised basaltic-andesitic phreatomagmatic tuff.</p> <p>The caldera-forming eruptions recorded by the Arran Volcanic Formation provide an important insight into caldera collapse processes and proximal ignimbrite successions. The lack of thick autobreccias and lithic-rich lapilli- and block-layers indicates that subsidence was relatively gradual and incremental in this caldera, and not accompanied by catastrophic wall collapse during eruption. The relatively horizontal nature of the caldera-fill units and paucity of intra-caldera faulting, indicate piston subsidence was the dominant method of collapse, with a relatively coherent caldera floor bounded by a steeply-dipping ring fault. Possible resurgence may have caused later doming of the floor and radial distribution of subsequent ignimbrites and sedimentary rocks. Our work emphasises the continued need for field studies of caldera volcanoes.</p>	
<b>Response to Reviewers:</b>	Editor comments	

	<p>Keywords: These have been changed to better reflect the specifics of the paper</p> <p>“The necessary addition is a better setting of your work in general context...” Additions have been made to the Abstract (lines 12-18), Introduction (lines 51-96), and the discussion (lines 518-542), with a final sentence at the end of the Conclusions (lines 637-640). References to other studies have been added throughout the discussion, in order to better set this work in the context of modern global studies.</p> <p>“Please, in the figures, also add the numbers to the scale bars and in the caption state how long the hammer is.” These have been done for all figures</p> <p>“Please also add labels to the features named in the photos in the figure captions” This has been done in all relevant figures.</p> <p>“Please also check the referencing” This has been done, largely thanks to your suggestions, and is now consistent throughout.</p>
<p><b>Author Comments:</b></p>	<p>Dear Editor,</p> <p>We wish to submit our revised manuscript, now entitled "A proximal record of caldera-forming eruptions: the stratigraphy, eruptive history, and collapse of the Palaeogene Arran caldera, western Scotland". Your comments were helpful, and we all feel the manuscript has been greatly improved.</p> <p>Sincerely</p> <p>Bob Gooday</p>

Table 1

Unit	Locations	Description	Interpretation
<u>Mulleann Gaoithe</u> Member [translation: <i>windmill</i> ]]	Mulleann Gaoithe in far NE of complex (extra-calderal). Dereneach in the far W of the complex.	<i>Lithologies:</i> Massive rhyolite (77-79 wt.% SiO <sub>2</sub> ) tuff. Minor mLT and red weathered non-welded tuff. <i>Crystals and clasts:</i> Abundant quartz up to 2 mm. K-feldspar, plagioclase, Fe-Ti oxides. Clasts in mLT = sandstone, dolerite, rhyolite <i>Textures:</i> cm-scale flow banding in lower and upper parts. Sub-mm fabric defined by <1 mm to near-continuous elongate bands	Rhyolitic parataxitic to lava-like ignimbrite. Very high-grade ignimbrite of 'Snake River type' (Andrews and Branney, 2011). Rapid deposition from a high temperature, (>900°C) high-mass-flux pyroclastic density current from low fountaining eruption. mLT record pulses of higher explosivity. Red tuff [sT] represents upper surface of ignimbrite sheet in contact with atmosphere.
<u>Allt Ruadh</u> Member [translation: <i>red stream</i> ]]	Western slopes of Ard Bheinn. Lower Glen Craigag.	<i>Lithologies:</i> Orange- and grey-weathering mLT. Minor crystal-rich and glassy tufts. <i>Crystals and clasts:</i> pre-Palaeogene schist, sandstone, quartzite. Palaeogene basalt, dolerite, occasional granite. Crystal tufts contain feldspar and minor quartz <i>Textures:</i> mLT massive. Crystal tufts are eutaxitic to lava-like.	Lithic-lapilli-rich non-welded ignimbrite deposited from a PDC at a flow-boundary zone dominated by fluid-escape, with very little turbulent shear-induced tractional segregation (Branney and Kokelaar, 2002). Highly explosive, caldera-forming eruptive phase. mTr record phases of lower explosivity.
<u>Creag Shocach</u> Conglomerates [translation: <i>snout crag</i> ]]	Western slope of Ard Bheinn. Creag Shocach above Glenloig.	<i>Lithologies:</i> Red conglomerates, breccias, and minor sandstones <i>Crystals and clasts:</i> Pre-Palaeogene medium- to coarse-grained red sandstones and quartzite conglomerates. Fine to medium sand matrix. <i>Textures:</i> Clast supported and matrix supported in different areas.	Erosion of Devonian and Permo-Triassic lithologies from steep caldera walls left by caldera subsidence related to eruption of the Allt Ruadh Member. Deposition – alluvial/fluvial.
<u>Creag an Fheidh</u> Member [translation: <i>deer crag</i> ]]	Creag an Fheidh. E of Creag Shocach.	<i>Lithologies:</i> glassy mT, mTr, and mLT <i>Crystals and clasts:</i> Crystals largely feldspar, with lesser quartz. Clasts in mLT of rhyolite and sedimentary rocks. Upper surface contains rounded pebbles and cobbles of rhyolite and quartzite. <i>Textures:</i> Some bedding-parallel flow-fabric in glassy units. Some mTr are eutaxitic	Heterogeneous ignimbrites recording a range of eruptive styles. mLT and mTr record variably highly-explosive eruptions and deposition from a PDC at a flow-boundary zone dominated by fluid-escape. Eutaxitic and glassy tufts record higher emplacement temperatures. Rounded clasts evidence for fluvial reworking on upper surface of ignimbrite.

<p><u>Allt Beith tuff cone</u> [translation: <i>birch stream</i>]</p>	<p>Near the head of the Allt Beith</p>	<p><i>Lithologies:</i> Finely laminated basaltic-andesitic (54.5 wt.% SiO<sub>2</sub>) tuff <i>Crystals and clasts:</i> None identified <i>Textures:</i> Planar bedding and cross-stratification. Some graded bedding.</p>	<p>Localised phreatomagmatic tuff cone – very fine grain size suggests intense fragmentation. Well-developed stratification suggests deposition from a fully dilute pyroclastic density current at a traction dominated flow boundary zone (Branney and Kokelaar 2002, Brown et al 2007).</p>
<p>White Tuff Member</p>	<p>Western slopes of Ard Bheinn. Plateau between Ard Bheinn and Glen Craigag.</p>	<p><i>Lithologies:</i> Massive rhyolite (76-77 wt.% SiO<sub>2</sub>) tuff with some autobreccia and conglomerate at top <i>Crystals and clasts:</i> Quartz and feldspar up to 2 mm. Upper conglomerate contains clasts of rhyolitic tuff, basalt, quartzite <i>Textures:</i> Largely massive with planar and chaotic flow banding in places</p>	<p>Rhyolitic lava-like ignimbrite. Very high-grade ignimbrite of 'Snake River type' (Andrews and Branney, 2011). Rapid deposition from a high temperature, (&gt;900°C) high-mass-flux pyroclastic density current from low fountaining eruption. Autobreccia may record post-deposition slumping. Upper conglomerate evidence for fluvial reworking on upper surface of ignimbrite.</p>
<p>Pigeon Cave Member</p>	<p>Slopes of Binnain na h-Uaimh. E of Glen Craigag.</p>	<p><i>Lithologies:</i> Turquoise-weathering mLT and mAg with minor glassy mT <i>Crystals and clasts:</i> Quartz and less abundant feldspar and Fe-Ti oxides. Clasts of pre-Palaeogene schist and sandstone and Palaeogene basalt and rhyolite. Lava-like cognate spatter clasts. <i>Textures:</i> Some bedding-parallel fabric in glassy units. Cognate spatter clasts are elongate ribbons.</p>	<p>Heterogeneous ignimbrites recording highly dynamic and fluctuating deposition history. mT and mLT formed as above. mAg formed from rapid deposition of cognate clasts (with lithic lapilli) from a pyroclastic density current rich in ash and dominated by fluid escape (Branney and Kokelaar, 2002).</p>
<p><u>Binnain na h-Uaimh</u> conglomerates [translation: <i>hill of the caves</i>]</p>	<p>Northern slopes of Binnain na h-Uaimh.</p>	<p><i>Lithologies:</i> Very coarse conglomerate. <i>Crystals and clasts:</i> Pebbles to large cobbles of sandstone and schist (resemble local Dalradian units) and smaller pebbles of vein quartz and quartzite. <i>Textures:</i> Clast supported. No clast alignment.</p>	<p>Debris flow conglomerate recording mass wasting of surrounding landscape into caldera.</p>
<p><u>Ard Bheinn Member</u> [translation: <i>high peak</i>]</p>	<p>Summits of Ard Bheinn and Binnain na h-Uaimh.</p>	<p><i>Lithologies:</i> Dominated by glassy rhyolitic (77 wt.% SiO<sub>2</sub>) mT and mTcr. Minor autobreccias, agglomerates, and lapilli tuff. Purple-grey units near top are dacitic (68-70 wt. % SiO<sub>2</sub>)</p>	<p>Mostly lava-like ignimbrites. Lower part of unit (to 440 m) is thought to represent one single eruption event, with hot (&gt;900°C) ash deposited from a pyroclastic density current at</p>

		<p><i>Crystals and clasts:</i> Crystals in mTcr are primarily plagioclase. Coarse crystal tuff at base contains large resorbed quartz and less abundant feldspars.</p> <p><i>Textures:</i> Largely vitrophyric with platy flow fabric in places. Agglomerates show distinct banding. Lapilli tuff near top is eutaxitic with flame of mafic material.</p>	<p>a relatively stable flow-boundary zone. Continuous jointing throughout suggests one single cooling unit. Upper parts of the member (above 440 m) likely formed from a series of small pyroclastic fountain eruptions of varying temperature, recording deposition at an unstable flow-boundary zone. Agglomerates deposited rapidly from a proximal pyroclastic density current.</p>
--	--	---	---

Table 2

Symbol	Meaning	Example Lithofacies
m	massive	mT - massive tuff
s	stratified	sLT - stratified lapilli tuff
db	diffusely bedded	dbTcr - diffusely bedded crystal-rich tuff
L	lapilli	mLT - massive lapilli tuff
T	tuff	mT - massive tuff
Br	breccia	mBr - massive breccia
Ag	agglomerate	mLAg - massive lapilli agglomerate
l-l	lava-like	mTl-l - massive lava-like tuff
cr	crystal-rich	mTcr - massive crystal-rich tuff
v	vitrophyric	mTv - massive vitrophyric tuff
e	eutaxitic	mLTe - massive eutaxitic lapilli tuff

Table 3

Sample Unit	BJG/15/95 Allt Beith	BJG/15/78 Ard Bheinn	BJG/15/133 Ard Bheinn	BJG/15/135 Ard Bheinn	BJG/15/31 Mulleann Gaoithe	BJG/17/3 Mulleann Gaoithe	BJG/17/23 Mulleann Gaoithe	BJG/15/8 White Tuff	BJG/15/14 White Tuff
Easting	194494	194504	194276	194335	198373	198490	198376	193937	194242
Northing	633982	632829	633467	633297	635029	634980	634970	632857	632457
SiO <sub>2</sub>	54.50	67.82	77.00	69.95	76.89	78.39	78.97	77.32	75.72
TiO <sub>2</sub>	0.92	1.18	0.53	0.77	0.08	0.07	0.07	0.10	0.11
Al <sub>2</sub> O <sub>3</sub>	25.30	13.26	9.94	12.31	12.30	12.29	12.54	12.62	12.63
FeO <sup>T</sup>	13.89	7.63	4.21	7.13	1.84	1.20	1.22	1.68	1.73
MnO	0.11	0.25	0.15	0.14	0.09	0.03	0.03	0.07	0.09
MgO	0.18	0.67	1.93	0.80	0.36	0.07	0.07	0.12	0.01
CaO	0.46	3.21	1.39	1.22	0.29	0.17	0.18	0.34	0.34
Na <sub>2</sub> O	2.52	3.48	2.11	3.88	2.88	2.47	2.52	2.56	2.44
K <sub>2</sub> O	2.97	2.84	2.96	3.26	4.95	5.54	5.65	5.22	6.49
P <sub>2</sub> O <sub>5</sub>	0.24	0.30	0.09	0.10	0.01	0.03	0.03	0.03	0.01
Total	101.10	100.65	100.32	99.56	99.70	100.25	101.27	100.07	99.58
LOI	2.10	0.59	1.00	1.40	0.71	1.15	1.15	0.97	0.90

[Click here to view linked References](#)

1 **A proximal record of caldera-forming eruptions: the stratigraphy,**  
2 **eruptive history, and collapse of the Palaeogene Arran caldera,**  
3 **western Scotland**

4 Robert J. Gooday<sup>1</sup>, David J. Brown<sup>2</sup>, Kathryn M. Goodenough<sup>3</sup>, Andrew  
5 C. Kerr<sup>1</sup>

6 1: School of Earth and Ocean Sciences, Cardiff University, Main Building, Park Place, Cardiff  
7 CF10 3AT, UK

8 2: School of Geographical and Earth Sciences, University of Glasgow, Gregory Building, Lilybank  
9 Gardens, Glasgow G12 8QQ, UK

10 3: British Geological Survey, The Lyell Centre, Edinburgh EH14 4AP, UK

11

12 **Abstract:** Caldera-forming volcanic eruptions are among the most dangerous, and can  
13 generate extensive pyroclastic deposits and deliver ash into global atmospheric  
14 circulation systems. As calderas collapse, the eruptions can deposit thick proximal  
15 ignimbrite sequences and thinner ignimbrites more distally. However, the proximal  
16 record of caldera collapse is often obscured by later intrusions, volcanism, faults,  
17 alteration, water and sediments, which significantly limits our understanding of these  
18 eruptions.

19 A Palaeogene caldera system in central Arran, western Scotland, preserves a rare  
20 proximal caldera-fill succession, the Arran Volcanic Formation. This caldera largely  
21 comprises highly heterogeneous ignimbrites and minor intra-caldera sedimentary rocks.  
22 The current level of erosion, and the general absence of faults, intrusions and  
23 sediments, allows a complex stratigraphy and collapse history to be determined, which  
24 can be linked to changing eruptive styles at a constantly-evolving volcano.



25 The first recorded phase was eruption of a homogeneous rhyolitic lava-like tuff,  
26 deposited from high temperature, high mass-flux pyroclastic density currents generated  
27 from low fountaining columns that retained heat. A succeeding phase of highly  
28 explosive Plinian eruptions, marked by a thick blanket of massive lapilli tuffs, was then  
29 followed by piston-like caldera collapse and erosion of steep caldera walls. Volcanism  
30 then became generally less explosive, with predominantly lava-like and eutaxitic tuffs  
31 and cognate-spatter-rich agglomerates interbedded with non-homogenous lapilli tuffs.  
32 High topographic relief between distinct units indicate long periods of volcanic  
33 quiescence, during which erosive processes dominated. These periods are, in several  
34 places, marked by sedimentary rocks and evidence for surface water, which includes a  
35 localised basaltic-andesitic phreatomagmatic tuff.

36 The caldera-forming eruptions recorded by the Arran Volcanic Formation provide an  
37 important insight into caldera collapse processes and proximal ignimbrite successions.  
38 The lack of thick autobreccias and lithic-rich lapilli- and block-layers indicates that  
39 subsidence was relatively gradual and incremental in this caldera, and not accompanied  
40 by catastrophic wall collapse during eruption. The relatively horizontal nature of the  
41 caldera-fill units and paucity of intra-caldera faulting, indicate piston subsidence was the  
42 dominant method of collapse, with a relatively coherent caldera floor bounded by a  
43 steeply-dipping ring fault. Possible resurgence may have caused later doming of the  
44 floor and radial distribution of subsequent ignimbrites and sedimentary rocks. Our work  
45 emphasises the continued need for field studies of caldera volcanoes.

46

47 **Keywords:** caldera collapse, resurgence, pyroclastic, lava-like ignimbrites, eruptive  
48 history

49

## 50 **Introduction**

51 Calderas are the surface expressions of complex volcano-magmatic systems, with  
52 prolonged periods of unrest and eruption (Acocella et al., 2015; Nobile et al., 2017)  
53 punctuated by extensive periods of quiescence. Although much debated, caldera  
54 collapse is typically caused by the withdrawal of large volumes of magma from shallow  
55 magma chambers (Druitt and Sparks, 1984; Lipman, 1997; Cole et al., 2005; Cashman  
56 and Giordano, 2014), and subsidence of a coherent block of crust into the  
57 underpressurised chamber(s) (Mori and McKee, 1987; Lipman, 1997, Cole et al., 2005;  
58 Acocella 2007), although collapse may also be triggered by overpressure within the  
59 chamber initiating fractures in the roof rocks (Gudmundsson, 1988; 1998). Caldera-  
60 forming eruptions are typically silicic and can deposit extensive sheets of ignimbrite  
61 both within and beyond the collapse caldera, together with widespread fall deposits,  
62 and even the circulation of ash globally (e.g. Self and Rampino, 1981; Self et al., 1984;  
63 Newhall and Dzurisin 1988; Hildreth and Fierstein, 2012).

64 Understanding caldera-forming eruptions and syn-eruptive collapse mechanisms is  
65 notoriously difficult at both modern and ancient calderas. Monitoring unrest at active  
66 calderas using seismic and remote sensing methods is essential in forecasting volcanic  
67 activity, but understanding these relationships is complex. How much magma  
68 withdrawal is required to induce collapse and how does collapse vary (Geshi and  
69 Miyabuchi, 2016)? Furthermore, how many collapse events may occur in the lifecycle of  
70 a caldera (e.g. due to evacuation of multiple magma reservoirs), and how might the  
71 deposits of these different eruption and collapse events vary both temporally and  
72 spatially (proximal and distal)? Answering these questions at active calderas is  
73 challenging, as only the latest stages in the caldera's deposits and structures are  
74 preserved and access may be further obscured by water and sediments (Acocella, 2007).

75 Therefore, we can look to ancient and more recent but inactive calderas. There are  
76 numerous field studies of such calderas (see reviews by Cole et al., 2005; Cashman and  
77 Giordano, 2014) that attempt to resolve questions on caldera collapse and evolution,  
78 and these have been supported more recently by numerical and analogue modelling  
79 studies (e.g. Troll et al., 2002; Acocella, 2007; Geshi et al., 2012). However, ancient  
80 calderas can typically be obscured by resurgent intrusions and volcanic deposits,  
81 thoroughly disrupted by faults and hydrothermal alteration, and/or obscured by water  
82 and later sediments. The level of erosion and preservation of the volcanic deposits and  
83 caldera-controlling structures can also represent a particular constraint to study. These  
84 constraints are particularly important with respect to the intra-caldera/proximal records  
85 of eruption, which are consequently less well studied than more distal, better preserved  
86 ignimbrite sheets (Smith and Kokelaar, 2013).

87 Therefore, it remains a challenge to volcanologists to identify ancient calderas where  
88 access and preservation allow for detailed field observations that can be used to  
89 elucidate caldera collapse and caldera-forming eruption processes. We argue that,  
90 given modern advances in physical volcanology (in particular pyroclastic density  
91 currents, the sedimentation of ignimbrites, and better understanding of lava-like  
92 ignimbrites; e.g. Branney and Kokelaar, 2002; Branney et al., 2008; Brown and Branney,  
93 2013), it is therefore essential to revisit localities that have not received recent  
94 attention. In this paper, we present a field study of a Palaeogene caldera system on the  
95 Isle of Arran, western Scotland, as an example of the proximal record of caldera-forming  
96 eruptions and the nature of collapse within the caldera.

### 97 **Why the Isle of Arran?**

98 The Isle of Arran in the Firth of Clyde, western Scotland, hosts some well-preserved  
99 remnants of the British Palaeogene Igneous Province (Fig. 1). The British Palaeogene  
100 Igneous Province itself is part of the North Atlantic Igneous Province, a predominantly

101 mafic Large Igneous Province that developed during the rifting of the North Atlantic  
102 Ocean in response to the arrival of the Iceland plume at the base of the lithosphere  
103 (e.g., Thompson and Gibson, 1991; Kent and Fitton, 2000; Storey et al., 2007). In the  
104 British Isles the North Atlantic Igneous Province comprises the extensive lava fields of  
105 Skye, Eigg, Mull-Morvern, and Antrim (Emeleus and Bell, 2005), as well as localised  
106 intrusive and volcanic centres (Fig. 1), including Arran. Other Palaeogene remnants of  
107 the North Atlantic Igneous Province are preserved on Greenland, the Faroe Islands, and  
108 offshore (Saunders et al., 1997). Although the majority of magmatism in the British  
109 Palaeogene Igneous Province is preserved as basaltic lavas and gabbroic and granitic  
110 intrusions, there is widespread evidence of extrusive silicic volcanism and explosive  
111 eruptions (Bell and Emeleus, 1988; Brown et al., 2009). Due in part to its historical  
112 importance and relative ease of access, the British Palaeogene Igneous Province has  
113 been the source of many developments in the global understanding of volcanological  
114 processes.

115 Pyroclastic rocks in the British Palaeogene Igneous Province are largely found within  
116 calderas (on Mull and Rùm, as well as Skye and Arran), often bound by arcuate faults  
117 and intrusions, originally interpreted as ring faults, ring dykes, and cone sheets.  
118 Detailed studies of the pyroclastic successions on Skye and Rùm have revealed complex  
119 histories of caldera collapse in the British Palaeogene Igneous Province (Troll et al.,  
120 2000; Holohan et al., 2009; Brown et al., 2009), but exposures in these areas are limited  
121 due to later, cross-cutting layered intrusions. Recently, many silicic extrusive rocks in  
122 this province, previously described as lavas or shallow intrusions, have been re-  
123 interpreted as welded and rheomorphic lava-like ignimbrites, for example the  
124 rhyodacite sheets on Rùm (Troll et al., 2000; Holohan et al., 2009) and the Sgurr of Eigg  
125 Pitchstone (Brown and Bell, 2013). These studies have allowed us to better understand  
126 the processes at work in, and make comparison with, other lava-like ignimbrite-  
127 producing volcanic provinces, for example, the Snake River Plain (Knott et al., 2016), the

128 Paraná Magmatic Province (Luchetti et al., 2017), and the Canary Islands (Sumner and  
129 Branney, 2002).

130 Despite these advances in the region, the caldera system in central Arran has remained  
131 poorly studied. The caldera (approximately 9 km<sup>2</sup>) is well exposed in places, and  
132 contains a caldera-fill sequence of pyroclastic and minor sedimentary rocks. Critically, it  
133 has not been overly disrupted by alteration, faults, later intrusions and volcanic  
134 deposits, and the level of erosion is such that a relatively undisturbed sequence of the  
135 caldera stratigraphy and its structure is preserved. Therefore, this makes Arran an  
136 extremely important area in which to study volcanic and sedimentary processes, how  
137 these change through time and, in particular, proximal records of ignimbrite deposition  
138 at a caldera volcano, and its collapse mechanisms. Despite all these advantages, central  
139 Arran has been the subject of few studies since the work of King (1955).

140 By way of example, the historically active Öskjuvatn caldera at Askja, North Iceland, is a  
141 comparable size (around 12 km<sup>2</sup>) to the Arran caldera and occupies a similar tectonic  
142 (rift) setting (Trippanera et al., 2018). However, observations of the caldera-fill  
143 succession at Askja are impossible due to the presence of a large lake, and the only  
144 information on collapse processes during and following the 1875 eruption are from  
145 historical sources, which can be unreliable (Hartley and Thordarson, 2012). Given the  
146 similarities to such a nearby caldera that is close to significant population centres in  
147 Europe, we emphasise the need for detailed field study of localities such as Arran and  
148 the lessons that can be learned and applied to active calderas.

149 In this paper, we present new field and petrographic data from the pyroclastic rocks  
150 preserved in central Arran, propose a volcanological model for the formation, evolution,  
151 and collapse of the caldera, and discuss the nature of eruptions and proximal record of  
152 caldera-forming eruptions. We include discussion on what our analysis of this ancient  
153 centre shows in terms of large caldera-forming eruptions, their deposits, and resulting

154 structures in general.

## 155 **Geological setting**

156 The pre-Palaeogene rocks in the northern part of Arran (Fig. 1) comprise the  
157 Neoproterozoic to Lower Cambrian schists, phyllites, and grits of the Southern Highland  
158 Group (BGS, 1987), this being the youngest division of the Dalradian Supergroup  
159 (Stephenson et al., 2013). The pre-Palaeogene rocks in the southern half of the island  
160 are dominated by Devonian and Permo-Triassic red sandstones and conglomerates  
161 (containing clasts of quartzite, vein quartz, and schist – most likely eroded from an  
162 exposed Dalradian landscape), separated by a thin succession of Carboniferous  
163 sedimentary rocks and lavas (Fig. 1). The basement upon which these sedimentary rocks  
164 were originally deposited is not exposed. The Highland Boundary Fault, the major  
165 crustal lineament that separates the Dalradian rocks of the Grampian Terrane to the  
166 north from the Midland Valley Terrane to the south, is known to cross Arran (Fig. 1), but  
167 its exact trace is uncertain (Young and Caldwell, 2012).

168 The Palaeogene igneous rocks on Arran (Fig. 1) comprise the North Arran Granite, a  
169 caldera system in the centre of the island, and a suite of sills and minor intrusions in the  
170 south of the island, which vary in composition from dolerite to rhyolite. In addition, a  
171 mafic dyke swarm is exposed largely around the coast of the island and in the  
172 mountains in the north of the island (BGS, 1987). These dykes intrude the Dalradian  
173 meta-sedimentary rocks, the Palaeozoic and Mesozoic sandstones, and the Palaeogene  
174 intrusions (Tyrell, 1928; BGS, 1987). The North Arran Granite is a roughly circular  
175 laccolith that was likely intruded from the south or south-east (Stevenson and Grove,  
176 2014), suggesting that its emplacement could have been structurally controlled by the  
177 Highland Boundary Fault. It has been dated by  $^{40}\text{Ar}-^{39}\text{Ar}$  at  $57.85\pm 0.15$  Ma (Chambers,  
178 2000). Composite sills, with mafic margins and more evolved cores, are common across

179 much of southern Arran (Tyrell, 1928; BGS, 1987). The most well-known of these forms  
180 cliffs and coastal outcrops at Drumadoon Point (Fig. 1), and this intrusion, and adjacent  
181 dykes, have been dated at  $59.04 \pm 0.13$  Ma and  $59.16 \pm 0.17$  Ma (Meade et al., 2009). In  
182 this contribution, the Palaeogene caldera system in central Arran is named the Central  
183 Arran Igneous Complex, while the pyroclastic and sedimentary intra-caldera succession  
184 is termed the Arran Volcanic Formation.

185 The Central Arran Igneous Complex includes a series of pyroclastic rocks and coarse  
186 grained intrusions, and is approximately 4 km  $\times$  5 km in area. It was first mapped by  
187 Gunn et al. (1901) and has historically been known as the 'Arran Central Ring Complex'.  
188 This term was first used in the Arran Memoir (Tyrell, 1928), in which comparisons were  
189 drawn between the granitic intrusions around the edge of the complex and the Loch Bà  
190 felsite on Mull, which was interpreted as a caldera bounding ring dyke (Bailey et al.,  
191 1924). The complex sits within Devonian red sandstones (to the north and south) and  
192 Permo-Triassic red sandstones (to the west and east) (BGS, 1987). The volcanoclastic  
193 rocks of the caldera-fill sequence mostly crop out on and around the summit of Ard  
194 Bheinn (Fig. 2). King (1955) mapped the western part of the Central Arran Igneous  
195 Complex in detail and suggested that it was younger than the North Arran Granite, due  
196 to the fact that it appears to have been emplaced into sedimentary rocks that were  
197 previously domed during emplacement of the North Arran Granite, around 2 km to the  
198 north.

199 The 'vent agglomerates' (Tyrell, 1928) of the complex (interpreted here as lapilli tuffs  
200 and breccias) were originally thought to represent the products of a single explosive  
201 volcanic phase, which was followed by intrusion of 'felsites', and the growth of small  
202 resurgent volcanic edifices on the caldera floor (Gregory and Tyrell, 1924; Tyrell, 1928;  
203 King, 1955). Large outcrops of basalt, dolerite, and 'basalt breccia' were interpreted as  
204 the only remains of a Palaeogene lava pile that once covered Arran, which had collapsed

205 into the vent during subsidence (King, 1955). This caldera-collapse has also been  
206 proposed to explain the origin of the isolated exposures of Mesozoic sedimentary rocks  
207 in the complex (King, 1955). The intrusions, which comprise granites, gabbros, and  
208 intermediate hybrids, were thought to be mostly younger than the caldera-fill sequence  
209 based on poorly exposed field relationships (King, 1955, 1959). King (1955) also  
210 discussed differences within the agglomerates, noting that some seemed to be  
211 sedimentary in origin ('sedimentary agglomerates') or different in colour due to  
212 compositional variation ('andesitic and basaltic agglomerates').

## 213 **Sampling and Methods**

214 Fieldwork was carried out on Arran across several field seasons between 2015 and 2017.  
215 Most of the information presented in this paper is the result of detailed mapping and  
216 stratigraphic logging, however a number of samples were collected for thin section  
217 petrography and geochemical analysis. Only ignimbrite samples that we judged to be  
218 representative of magmatic compositions (i.e., clast-free) were subjected to whole-rock  
219 geochemical analyses.

220 Nine samples of clast-free ignimbrite from four units were crushed in a manganese-steel  
221 jaw-crusher and ground to a fine powder in an agate planetary-ball mill. Loss on Ignition  
222 (at 900 °C) was determined gravimetrically, before the samples were prepared using the  
223 methods outlined in McDonald and Viljoen (2006) at Cardiff University (UK). Major  
224 element analyses were carried out using inductively coupled plasma optical emission  
225 spectrometry (ICP-OES). Accuracy was constrained by subjecting the international  
226 reference materials BIR-1 (basalt) and JG-3 (granodiorite) to the same process. Precision  
227 was constrained by duplicates of unknown samples – duplicates generally provided  
228 uncertainties of <5% for elements with concentrations >2 wt%.

## 229 **The Central Arran Igneous Complex**



230 As part of the present study, the western half of the Central Arran Igneous Complex has  
231 been re-mapped (Fig. 2). The most fundamental difference between this new map and  
232 those of Tyrell (1928) and King (1955) is the lack of a near-complete ring intrusion. This  
233 complex, therefore, should not be described as a 'ring complex'. Although exposure of  
234 the caldera-fill rocks on the slopes of Ard Bheinn and Binnein na h-Uaimh (Figs 2, 3) is  
235 good, exposure in the majority of the rest of the complex is limited and largely restricted  
236 to stream beds. There is no exposure of a ring fault surrounding the complex, but the  
237 juxtaposition of Palaeogene igneous rocks at the same level as Palaeozoic sedimentary  
238 rocks indicates extensive downfaulting of the complex.

### 239 **Intrusive rocks of the Central Arran Igneous Complex**

240 The north and east of the complex (Figs. 1, 2), are dominated by the pre-caldera  
241 Glenloig Hybrids, named after the most accessible exposure under the bridge at  
242 Glenloig. They include texturally heterogeneous amphibole-bearing, fine-grained  
243 intermediate rocks, which vary in composition from basaltic-andesitic to dacitic, and  
244 lesser amounts of coarser grained granite and amphibole granite. These rock types  
245 display intrusive and mingling interaction textures with one another. In some stream  
246 sections, isolated exposures of quartz-bearing gabbro are found, however, due to poor  
247 exposure, it is not possible to deduce the relationship of these gabbros with the Glenloig  
248 Hybrids. A small outcrop of these Glenloig Hybrids, along with a thin outcrop of gabbro,  
249 is preserved as an inlier within the caldera-fill succession between Binnein na h-Uaimh  
250 and Creag Mhor (Figs 2, 3).

251 Several granitic bodies are found within the Central Arran Igneous Complex. The largest  
252 of these is the Glen Craigag Granite, which is mostly exposed in the upper parts of Glen  
253 Craigag and Ballymichael Glen, in the centre of the complex (Fig. 2). Its mineralogy  
254 principally comprises medium-grained quartz and perthitic K-feldspar, commonly in  
255 granophyric intergrowths, with minor plagioclase, amphibole, and accessory minerals. In

256 Ballymichael Glen, pyroclastic rocks overlie the Glen Craigag Granite on an eroded  
257 palaeosurface, suggesting intrusion and erosion of the granite occurred prior to the  
258 onset of explosive volcanism.

259 Several smaller granitic bodies crop out around the margins of the Central Arran Igneous  
260 Complex (Fig. 2). These are here collectively termed the Satellite Granites, and all  
261 comprise medium- to coarse-grained quartz, K-feldspar and plagioclase, with minor  
262 amphibole and biotite, and accessory minerals. They were originally mapped as a near-  
263 continuous 'ring intrusion' (Tyrell, 1928), but our mapping shows that they are isolated  
264 from one another at this level of erosion. Relationships to the other units of the Central  
265 Arran Igneous Complex are poorly exposed, but the Creag Mhor Granite appears to be a  
266 shallowly eastward dipping sheet within the ignimbrites, and the granite in Ballymichael  
267 Glen has steeply-dipping, complex contacts, with fingers protruding into the rocks of the  
268 Arran Volcanic Formation. This suggests that the granites intruded the lower pyroclastic  
269 units of the Arran Volcanic Formation. Their arrangement around the margins of the  
270 caldera could be a result of intrusion along a caldera-bounding ring fault.

271 A large outcrop of fine-to-medium grained basaltic rock on the western slopes of Ard  
272 Bheinn and Binnein na h-Uaimh (Figs 2, 3) was originally interpreted as the only remnant  
273 of an inferred Arran lava field, that had subsided into the caldera (King, 1955).

274 Petrographic work during this study shows that it is, for the most part, an ophitic  
275 dolerite. Mineralogy is consistent throughout the outcrop, and consists of small  
276 plagioclase laths, commonly embedded in clinopyroxene oikocrysts up to 3 mm in size,  
277 and patches of iddingsite show alteration of primary olivine. This unit displays a clear  
278 intrusive relationship with several of the pyroclastic units of the Arran Volcanic  
279 Formation, with small fingers of dolerite intruding into the overlying unit (White Tuff  
280 Member). In many places, especially near the contacts, the dolerite is heavily  
281 brecciated, with peperitic textures visible in several exposures. There is also one small

282 outcrop of the underlying unit (Allt Ruadh Member) preserved above it. Other than this,  
283 it is largely concordant with stratigraphy (Figs. 2, 3), so we interpret the unit as a sill.

284 A suite of mafic dykes, largely <2 m wide and similar in morphology and composition to  
285 the dykes exposed all over Arran, intrudes the Glenloig Hybrids, the Glen Craigag  
286 Granite, and the lowest extra-caldera ignimbrites (the Muileann Gaoithe Member) (Fig.  
287 2). No mafic dykes are observed intruding the Satellite Granites or the caldera-fill  
288 succession of the Arran Volcanic Formation. The only dyke seen intruding an intra-  
289 caldera ignimbrite is a pitchstone (i.e., silicic and vitrophyric) dyke in a tributary to the  
290 Glen Craigag stream.

## 291 **The Arran Volcanic Formation**

292 The caldera-fill succession is made up dominantly of pyroclastic rocks, with some minor  
293 sedimentary packages. We assign all these rocks, as well as pyroclastic units that were  
294 deposited outside the caldera, to the Arran Volcanic Formation.

295 The Arran Volcanic Formation comprises a number of different mappable pyroclastic  
296 units which we interpret as ignimbrites (i.e., the deposits of pyroclastic density currents)  
297 (Fig. 2), separated by erosional unconformities and sedimentary horizons. They are best  
298 exposed in the western third of the complex (i.e., west of Glen Craigag; Fig. 2), with  
299 good exposure on the high ground around Ard Bheinn and Binnein na h-Uaimh (Fig. 3).  
300 This is the area that King (1955) described in detail. Exposures of these rocks are found  
301 over an elevation change of more than 400 m (Fig. 3), giving the best estimate of total  
302 preserved thickness. Dips of units and other structural data are impossible to measure  
303 due to the lack of bedding seen at the scale of individual exposures. Where a sense of  
304 dip can be gleaned from following contacts, beds appear approximately horizontal.  
305 Away from a small number of outcrops showing a possible caldera basement, it is  
306 impossible to estimate how far the Arran Volcanic Formation extends below the level of

307 exposure. An unknown thickness of the Arran Volcanic Formation above the current  
308 level of exposure has been lost to erosion.

309 The general volcanic stratigraphy of the area is shown in Fig. 4, with stratigraphic and  
310 lithological information displayed in Table 1. We assign the mappable pyroclastic units  
311 as individual members within the Arran Volcanic Formation, based on lithological  
312 variations between units, and the presence of mappable palaeotopographic surfaces.  
313 The general characteristics of each member (weathering colour, lithology, clast  
314 composition, *etc.*) are generally distinct enough to allow isolated exposures to be  
315 assigned to the appropriate unit. However, the upper surfaces of all members show  
316 evidence for fluvial reworking, erosion, deposition of sedimentary units, and/or  
317 prolonged contact with the atmosphere (Fig. 4), which all suggest volcanic hiatuses.  
318 Reddened units are tentatively used to identify either distinct members or inter-  
319 member eruptive/flow units whose surfaces have undergone prolonged exposure to the  
320 atmosphere (no features of true palaeosols such as rootlets or bioturbation were  
321 identified). Within members, deposition is assumed to be sustained with lithological  
322 differences reflecting variations in mass-flux and temperature during progressive  
323 aggradation of the ignimbrite (Branney and Kokelaar 2002). Within certain members,  
324 cooling joints are used to identify distinct cooling units. The terminology used to  
325 describe the different lithofacies mapped here is given in Table 2 and follows the  
326 lithofacies code approach of Branney and Kokelaar (2002).

### 327 **The Muileann Gaoithe Member**

328 This is the lowest exposed unit within the caldera (Fig. 4), and is the only volcanic unit  
329 exposed outside the caldera. A stratigraphic log up the extra-caldera Muileann Gaoithe  
330 section is shown in Fig. 5a. It largely comprises a white-weathering flow-banded rhyolite  
331 tuff (77-79 wt.% SiO<sub>2</sub>, Table 3) with some layers of massive lapilli tuff (mLT) and thinly  
332 bedded red tuff (sT). In places near the base the flow banding displays metre-scale

333 folding (Fig. 5b). Abundant smoky quartz crystals up to 2 mm are characteristic of this  
334 unit. The glassy groundmass shows sub-mm (Fig. 5c) to continuous (Fig. 5d)  
335 compositionally distinct bands.

336 We interpret the Muileann Gaoithe Member as a rhyolitic parataxitic to lava-like  
337 ignimbrite. The layers of lapilli tuff may represent changes in flow-boundary conditions  
338 within the aggrading ignimbrite, which could reflect increased explosivity at the vent.  
339 The red tuff is thought to represent ash which capped the underlying eruptive unit and  
340 was exposed to the atmosphere before deposition of the overlying unit. This would  
341 separate the Muileann Gaoithe section into two eruptive units, each capped by a thin  
342 red tuff. At Dereneneach, red tuff is only observed at the top of the unit, suggesting only  
343 one eruptive unit is exposed here.

#### 344 **The Allt Ruadh Member**

345 The stratigraphy of the Allt Ruadh Member along the Allt Ruadh section is shown in Fig.  
346 6a. It is dominated by orange- and grey-weathering massive lithic-lapilli tuffs (mLT; Fig.  
347 6b), containing clasts of pre-Palaeogene schist, sandstone, and quartzite, and  
348 presumably Palaeogene basalt, dolerite, and occasional granite (Fig. 6c). Thin layers of  
349 high-grade crystal tuffs (Fig. 6d) are exposed in the lower part of the Allt Ruadh section.  
350 Elsewhere in the complex where exposure is not as good, only the mLT are seen.

351 We interpret this unit as a series of non-welded ignimbrites representing a prolonged  
352 period of highly explosive volcanism, in which a large volume of magma was erupted.  
353 The vitrophyric and eutaxitic layers are interpreted as phases of lower explosivity in  
354 which the pyroclastic density current retained more heat. The purple glassy tuffs near  
355 the top of the section (Fig. 6a) may be basal vitrophyres to the overlying packages of  
356 mLT.

#### 357 **Creag Shocach conglomerates**

358 The Creag Shocach conglomerates are a series of sandstones, gritstones, and  
359 conglomerates which overlie the Allt Ruadh Member (Fig. 4). They are 'mesobreccias' in  
360 the classification of Lipman (1976). The clasts (pebbles and cobbles) comprise pre-  
361 Palaeogene country rock lithologies, i.e., red sandstones and quartzite conglomerates.  
362 The matrix largely comprises fine- to medium-grained quartz sand. We interpret this  
363 unit as representing erosion of Devonian and Permo-Triassic lithologies into the caldera  
364 from steep caldera walls left by subsidence related to the eruption of the Allt Ruadh  
365 Member.

### 366 **Creag an Fheidh Member**

367 The Creag an Fheidh Member is only exposed in the east of the complex, and appears to  
368 be cut off by the same fault that truncates the intra-caldera outcrop of Glenloig Hybrids  
369 (Fig. 2). The lower parts of this unit (which are only well-exposed on Creag an Fheidh,  
370 and may not be laterally extensive) are predominantly lithic-poor tuffs and crystal tuffs  
371 (mT and mTcr) with some massive lapilli tuffs towards the top of the unit (Fig. 7a, b).  
372 Some of the crystal tuffs have a characteristically dark glass groundmass (Fig. 7c). In thin  
373 section, the eutaxitic tuffs show flattened wispy features interpreted as fiamme (Fig.  
374 7d). The massive lapilli tuff at the top of the unit contains abundant clasts of rhyolite  
375 which resemble the Muileann Gaoithe lava-like tuffs. The upper surface contains  
376 rounded pebbles and cobbles of rhyolite and quartzite.

377 The unit is interpreted as a series of localised heterogeneous ignimbrites that were only  
378 deposited in the eastern part of the complex. The increasing lithic lapilli content  
379 suggests the eruptions became more explosive with time. The rounded pebbles and  
380 cobbles and presence of exotic clasts at the top of the unit suggest fluvial reworking of  
381 the upper surface of the ignimbrite in a period of volcanic quiescence before the  
382 eruption of the White Tuff Member.

383 **Allt Beith tuff cone**

384 On the upper surface of the Creag an Fheidh Member are several exposures of a very  
385 fine brown-grey thinly banded tuff (Fig. 3). It shows both cross-stratified and planar  
386 bedding features on scales of <1-50 mm, with occasional graded bedding (Fig. 8). Unlike  
387 all other erupted products within the CAIC, it is basaltic-andesitic in composition (54.5  
388 wt.% SiO<sub>2</sub>; Table 3). The surrounding exposures are dominated by the conglomerates  
389 that make up the upper surface of the Creag an Fheidh ignimbrite. We interpret these  
390 exposures as the remnants of a small basaltic phreatomagmatic tuff cone or ring. This  
391 interpretation is based on four main features: 1) the deposit is very fine grained,  
392 suggesting intense fragmentation, 2) phreatomagmatism can explain explosive mafic  
393 activity and the production of fine basaltic-andesitic ash, 3) it is surrounded by other  
394 deposits of fluvial facies, and 4) it is very localised, being seen nowhere else in the  
395 complex.

396 **White Tuff Member**

397 The White Tuff is a very homogeneous, white-weathering rhyolitic tuff. Most exposures  
398 of this tuff appear structureless, although in places a distinct planar fabric can be seen  
399 (Fig. 9a). This is most often sub-horizontal planar banding, but in places it is chaotic.  
400 These fabrics are variably expressed as pervasive fractures tens of centimetres apart, or  
401 as fine mm-scale colour variations (Fig. 9b). The White Tuff Member is petrologically  
402 and geochemically homogeneous. It is rhyolitic throughout (76-77 wt. % SiO<sub>2</sub>; Table 3),  
403 containing abundant plagioclase, K-feldspar, and smoky quartz crystals 1-5 mm in size  
404 (Fig. 12c,d). The top of the unit comprises a localised conglomerate with rounded clasts  
405 of rhyolite, basalt, and quartzite. The White Tuff Member is interpreted as a voluminous  
406 rhyolitic lava-like ignimbrite. The conglomerate at its upper surface, which contains  
407 exotic clasts as well as cobbles of rhyolitic tuff, suggests fluvial working on the exposed

408 surface of the unit after deposition.

#### 409 **Pigeon Cave Member**

410 The Pigeon Cave Member comprises glassy tuffs, massive lapilli tuffs, and massive lapilli  
411 agglomerates (Fig. 10a,b). The agglomerates are characterised by weathering to a  
412 turquoise colour, and containing elongate ribbons of lava-like rhyolite (Fig. 10c),  
413 interpreted as deformed cognate spatter clasts. Many of the crystal tuffs have a distinct  
414 black glassy groundmass (Fig. 10d). Small spatter clasts can be recognised in thin section  
415 as wispy glassy features (Fig. 10e). The Pigeon Cave Member is interpreted as a series of  
416 heterogenous ignimbrites, with the massive lapilli tuffs recording highly explosive  
417 eruptions, and the agglomerates recording slightly less explosive spatter eruptions.

418 The outcrop of 'Cretaceous chalk' at Pigeon Cave on Binnein na h-Uaimh (discussed by  
419 Tyrell, 1928) is overlain by the Pigeon Cave Member and has been previously  
420 interpreted as a subsided megablock (Tyrell, 1928; King, 1955). Some pink-white  
421 weathering sandstones are exposed several metres to the south of Pigeon Cave. These  
422 were also mentioned by Tyrell (1928), and King (1955) suggested these may also be  
423 Cretaceous due to similarities with sediments found on Mull and Morvern, as well as in  
424 Antrim. It is unclear whether these sedimentary units are part of the caldera floor,  
425 subsided megablocks, or have a Palaeogene intra-caldera origin.

#### 426 **Binnein na h-Uaimh conglomerates**

427 The Binnein na h-Uaimh conglomerates comprise a number of exposures of very coarse  
428 clast-supported conglomerates (Fig. 4). The contact with the underlying Pigeon Cave  
429 Member can be traced for tens of metres down the northern side of Binnein na h-  
430 Uaimh, suggesting that flow was towards the north. In places this contact is steep, and is  
431 interpreted as the side of a canyon eroded into the underlying ignimbrites. The larger  
432 clasts are predominantly schist, which resembles the Dalradian schists exposed several



433 kilometres to the north, on the other side of the Highland Boundary Fault.

#### 434 **Ard Bheinn Member**

435 The Ard Bheinn Member is the youngest exposed volcanic unit in the Central Arran  
436 Igneous Complex (Fig. 4). It makes up the summit of Ard Bheinn, so anything above this  
437 level has been lost to erosion. Its lower parts are dominated by clast-poor glassy and  
438 crystal-rich tuffs (Fig. 11a) with some lithophysae and planar flow fabric. The upper  
439 section is less homogenous, with autobreccia, agglomerates (Fig. 11b), crystal tuffs (Fig.  
440 11c; the '*plagioclase porphyry*' of King, 1955), and eutaxitic lapilli tuffs (Fig. 11d). The  
441 lowest exposures of this member comprise stratified, lava-like, coarse crystal tuffs (Fig.  
442 11b) which appear to fill a valley eroded into the underlying units (Fig. 2). This valley can  
443 be traced towards the south, away from Ard Bheinn, suggesting that flow here was to  
444 the south.

445 The Ard Bheinn Member is interpreted as a series of high-grade ignimbrites – most  
446 being 'lava-like' on the basis of completely agglutinated pyroclasts (Fig. 11c, e). The  
447 lower part of the Ard Bheinn section (360 m to 440 m on Fig. 11a) displays consistent  
448 columnar jointing, suggesting that this section acted as a single cooling unit. The upper  
449 parts of the member were likely formed from a series of small pyroclastic fountaining  
450 eruptions of varying explosivity and emplacement temperature.

#### 451 **Bedded Tuffs**

452 Some isolated exposures around the upper parts of Ballymichael Glen comprise  
453 ignimbrites that display stratification and flow banding on a variety of scales. These are  
454 shown in Fig. 2. Due to their isolated nature, and poor exposure on flat, vegetated  
455 ground, it is impossible to discern their relationship with any other of the mapped units.  
456 For this reason, we cannot determine their position within the stratigraphy of the Arran  
457 Volcanic Formation.

## 458 **Discussion**

459 This work demonstrates that the Central Arran Igneous Complex represents a well-  
460 preserved caldera system filled by a pyroclastic succession at least 400 m thick, the  
461 Arran Volcanic Formation. A number of sequential mappable units have been  
462 recognised, most of which are preserved within a broadly circular area, interpreted as a  
463 caldera. We discuss the collapse of the caldera and the nature of proximal ignimbrites  
464 before presenting an eruption history.

### 465 **Collapse (and resurgence?) of the caldera**

466 Given that the Arran Volcanic Formation comprises Palaeogene surface-deposited rocks  
467 juxtaposed against Devonian and Permo-Triassic rocks, it must occupy a caldera which  
468 has experienced at least some degree of downfaulting and must therefore possess at  
469 least one ring fault. Although this fault is not exposed, the complex meets the other  
470 criteria of Brown *et al.*, (2009) for recognising a caldera in the British Palaeogene  
471 Igneous Province: (1) a collapse succession of breccias; and (2) evidence of subsidence  
472 (i.e., displacement relative to country rocks).

473 A transect from the western edge of the caldera to the summit of Binnein na h-Uaimh is  
474 relatively well exposed, and no significant breaks or duplications in stratigraphy are  
475 seen. This suggests that there is only one ring fault, i.e., at the contact between the  
476 Arran Volcanic Formation and the pre-Palaeogene sedimentary country rocks.

477 Experimental studies and their comparison to real examples suggest that a caldera that  
478 displays one outward-dipping reverse ring fault is likely to have experienced subsidence  
479 in the range of 100 m to 1 km (Acocella, 2007).

480 One fault is identifiable *within* the caldera (Fig. 2), but there are doubtless others. The  
481 change in stratigraphy across this fault suggests the sense of movement was 'down to

482 the east', but there is no way to determine the magnitude of displacement. This fault is  
483 radial to the caldera.

484 Given the presence of at least one radial fault, an element of piecemeal subsidence can  
485 be assumed (Moore and Kokelaar, 1998; Troll et al., 2002). However, there are no other  
486 places where the stratigraphy is noticeably disrupted at the scale of the available  
487 exposure, so this was clearly not a dominant collapse mechanism. There may also be an  
488 element of trapdoor subsidence (Lipman, 1997), as massive lapilli tuffs of the Allt Ruadh  
489 Member are exposed in the east of the complex at the same elevation as the summit of  
490 Ard Bheinn. This could suggest greater subsidence of the caldera to the west, but could  
491 also be explained by lateral changes in deposit thicknesses (Brown and Branney, 2013)  
492 or amount of erosion. There is no evidence of consistently inward-dipping beds, or  
493 significant evidence of slumping, so funnel-like subsidence has not occurred (e.g.  
494 Miyakejima, Japan – Geshi et al., 2012). Given the broadly horizontal nature of the  
495 caldera-fill units and the lack of significant intra-caldera faulting, the closest-  
496 approximated end-member subsidence style (by the classification of Lipman, 1997;  
497 Acocella, 2007) is piston subsidence, in which a coherent caldera floor is bounded by  
498 one or more steeply-dipping ring faults. It is uncertain whether the Arran caldera ring  
499 fault is a simple outward-dipping reverse fault (Stage 2, Acocella, 2007) or an inward  
500 dipping normal fault with volcanic deposits masking the internal earlier ring fault (Stage  
501 4, Acocella, 2007). However, the relatively simple stratigraphy and lack of disruption  
502 likely indicate an outward-dipping reverse fault, supporting rare field and seismic  
503 evidence from calderas such as Rabaul, Papua New Guinea (Mori and McKee, 1987;  
504 Saunders, 2001).

505 The upper two units described here – i.e., the Binnein na h-Uaimh conglomerates and  
506 the Ard Bheinn Member – show some evidence of flow-directions towards the edges of  
507 the caldera. This suggests that at this stage in the caldera's history, there was a palaeo-

508 topographic high roughly in the location of the current Ard Bheinn summit. We  
509 tentatively suggest that this could be evidence for resurgent doming in the period  
510 following the main Allt Ruadh-related collapse event. Following Troll et al. (2002),  
511 doming may also explain the presence of the radial fault described above, and the  
512 northerly transport of Dalradian clasts within the caldera. Uplift associated with caldera  
513 resurgence has been linked to shallow magmatic intrusion of sills/dykes and laccoliths.  
514 This process has been identified through magnetotelluric imaging on the island of Ischia  
515 (Bay of Naples, Italy), where some 800 m of uplift, accompanied by volcanic activity, has  
516 occurred (Di Giuseppe et al., 2017).

#### 517 **The nature of proximal ignimbrites**

518 The majority of ignimbrites in the Arran Volcanic Formation are high grade (lava-like to  
519 welded) with rarer low grade, non-welded examples. These ignimbrites are indicative of  
520 high temperature, high mass-flux pyroclastic density currents generated from low  
521 fountaining columns that retained heat (Branney and Kokelaar, 2002). The lava-like  
522 ignimbrites typically display pervasive base-parallel flow banding, indicative of syn-  
523 depositional rheomorphism (Andrews and Branney, 2011). There are relatively few  
524 examples of post-depositional rheomorphism such as extensive domains of contorted  
525 flow banding and refolded folds (Andrews and Branney, 2011), and a general absence of  
526 autobreccia. Together, this indicates there was little slumping, sliding, and ultimately  
527 brittle deformation of the cool(ing) ignimbrites (e.g. Moore and Kokelaar, 1998;  
528 Andrews and Branney, 2011).

529 Perhaps most noticeable is the general lack of lithic-rich lapilli- and block-layers in the  
530 ignimbrites. These types of breccias/lapilli-tuffs are commonly found in intra-caldera  
531 proximal ignimbrites and are typically linked to climactic subsidence events and  
532 associated caldera wall/floor destabilisation. Modern examples of such units include  
533 Ischia (75 ka, Brown et al., 2008) and Pantelleria (46 ka, Jordan et al., 2018) in Italy, and

534 Tenerife in Spain (273 ka, Smith and Kokelaar, 2013). The absence of these units on  
535 Arran indicates that whilst subsidence clearly occurred, it was not always catastrophic  
536 and that explosive caldera-forming eruptions can occur without such ‘tracers’ of caldera  
537 collapse.

538 Overall, the general absence of slumping/sliding ignimbrites and the paucity of collapse-  
539 related lithic breccias, support a gradual piston-like collapse of the caldera, with only  
540 minimal disruption by faulting and/or later resurgence. In many respects, the Arran  
541 caldera is remarkable for its incremental but consistent collapse and the relative  
542 stability of the caldera floor.

### 543 **Eruptive History**

544 We now present an overall model for the eruptive history and caldera evolution of the  
545 Central Arran Igneous Complex which is consistent with the observations described in  
546 this paper (Fig. 12).

547 1- The lava-like ignimbrites of the Muileann Gaoithe Member are preserved *in situ* and  
548 as clasts within the later ignimbrite units. As the base is not seen within the caldera, we  
549 cannot say whether this was the first stage of volcanism in the area. It is possible that it  
550 overlies the erupted products of earlier volcanism that are now buried.

551 2- A period of highly explosive eruptions formed the Allt Ruadh Member (Fig. 12a). This  
552 blanket of mLT covers the entire area of the caldera (Fig. 2).

553 3- This evacuation of magma caused underpressure in the underlying magma chamber  
554 and caused the caldera to collapse. Collapse at this stage was piston-like, with a  
555 coherent caldera floor moving along a single ring fault, although an element of trapdoor  
556 subsidence with thickening to the west *may* have occurred (see Acocella, 2007). The  
557 steep caldera walls left by the outward-dipping reverse ring fault collapsed, forming the

558 Creag Shocach conglomerates (Fig. 12a).

559 4- The Creag an Fheidh Member was erupted in the eastern part of the caldera (Fig. 2)  
560 and ponded against a radial fault (Fig. 12b). The presence of this fault could be due to  
561 some degree of resurgent doming (Troll *et al.*, 2002).

562 5- The upper part of the Creag an Fheidh Member was fluviually reworked in a period of  
563 volcanic quiescence. A small pulse of mafic magmatism interacted with this surface  
564 water and/or groundwater, and the resulting phreatomagmatic eruption built the Allt  
565 Beith tuff cone (Fig. 12b).

566 6- The rhyolitic lava-like ignimbrites of the White Tuff Member were erupted (Fig. 12c).  
567 These ignimbrites are lithologically and petrographically almost identical to the  
568 Muileann Gaoithe Member ignimbrites, but were erupted after a significant period of  
569 non-homogeneous lower-grade volcanism. This stratigraphy, of variable pyroclastic  
570 rocks stratigraphically 'sandwiched' between two thick rhyolite units is very similar to  
571 that observed at Sabaloka, Sudan (Almond, 1971). This eruption was followed by a  
572 period of volcanic quiescence in which the upper surface was reworked.

573 7- The Pigeon Cave Member was erupted (Fig. 12c), and intruded by a dolerite sill (Figs  
574 4, 10a). The nature of the pre-Palaeogene sedimentary rocks (Cretaceous chalk and  
575 possibly Cretaceous sandstone) is unclear as contacts are not exposed, but work on Rùm  
576 suggests that supposed intra-caldera 'megablocks' may in fact be broadly coherent  
577 pieces of caldera floor (Holohan *et al.*, 2009; see also Lipman, 1976). If this is the case  
578 on Arran, these caldera floor segments may have been exposed by subsidence-related  
579 faulting and/or resurgent doming (see below).

580 8- The intrusion of a dolerite sill, or overpressure from the underlying magma chamber,  
581 or both, caused resurgent doming to form a palaeo-topographic high (Fig. 12d) in the  
582 vicinity of the modern Ard Bheinn summit.

583 9- Debris flows comprising material from outside the caldera flowed away from this  
584 palaeo-high and were deposited as the Binnein na h-Uaimh conglomerates in steep-  
585 sided canyons eroded into the upper surface of the Pigeon Cave Member (Fig. 12d).

586 10- The heterogeneous high-grade ignimbrites of the Ard Bheinn Member were erupted  
587 (Fig. 12d). The lowest of these – coarse crystal tuffs – flowed away from the palaeo-high  
588 and were deposited in valleys eroded into the underlying members (Fig. 2).

589 11- An unknown thickness of the Ard Bheinn Member and any overlying units were lost  
590 to erosion.

## 591 **Conclusions**

592 The Central Arran Igneous Complex is a good example of a well-preserved caldera  
593 volcano, as previously established by King (1955), and provides an excellent opportunity  
594 to investigate an intra-caldera sequence. Its caldera-fill succession, the Arran Volcanic  
595 Formation, was eroded to a relatively shallow level, and generally escaped modification  
596 by later intrusions/volcanism and significant faulting. Given the erosion levels the intra-  
597 caldera sequence provides an outstanding record of proximal ignimbrite deposition,  
598 which is often unavailable at other ancient calderas that have been heavily intruded and  
599 faulted, or modern calderas that are filled with later sediments and/or water, and have  
600 not been incised sufficiently. Detailed mapping and field observations have allowed us  
601 to interpret the caldera-fill rocks in terms of a stratigraphic sequence of successive  
602 eruptive units, which had not previously been attempted. This stratigraphy allows us to  
603 propose a chronological model for the formation of the complex and infer the processes  
604 which occur as small predominantly silicic calderas collapse. The ignimbrites are  
605 accompanied by sedimentary rocks recording intra-caldera fluvial, mass flow, and  
606 lacustrine deposition, which attest to significant eruption hiatuses. The ignimbrites are  
607 preserved almost exclusively as intra-caldera units, with only one example, the

608 Muileann Gaoithe Member, found beyond the caldera. The general absence of extra-  
609 caldera ignimbrites elsewhere on Arran is presumably due to erosion.

610 The ignimbrites of the Arran Volcanic Formation are dominated by high grade lava-like  
611 and welded ignimbrites. The Allt Ruadh Member is the only surviving product of a  
612 highly explosive phase of eruptions and period of caldera collapse. The other members  
613 typically record rapid deposition from high temperature (>900°C), high-mass-flux  
614 pyroclastic density currents generated from low-fountaining columns that do not  
615 entrain much atmospheric air, and therefore retain large amounts of heat (Branney et  
616 al., 1992). The members do however, show considerable variation and typically  
617 transition from lithoidal and flow banded lava-like tuffs, through eutaxitic tuffs and  
618 cognate spatter-bearing agglomerates, to occasional poorly to non-welded lapilli-tuffs.  
619 These variations indicate that the pyroclastic density currents were sustained but  
620 unstable and subject to variations in mass-flux and temperature.

621 Although some examples are recorded, there is a general paucity of autobreccia, and  
622 this indicates that little slumping and sliding of cool(ing) high-grade ignimbrite units  
623 occurred during pauses in deposition (e.g. Moore and Kokelaar, 1998). Furthermore,  
624 lithic-rich lapilli- and block-layers are rare, indicative of a general absence of climactic  
625 subsidence events and associated caldera wall/floor destabilisation, which may be  
626 anticipated in intra-caldera proximal successions (e.g. Smith and Kokelaar, 2013).  
627 Together, these data suggest that although deposition occurred rapidly, caldera  
628 subsidence was relatively incremental and piston-like, and that eruption of high grade  
629 ignimbrites can occur without catastrophic collapse (see also Lavallée et al., 2006). In  
630 eruption hiatuses, however, subsidence continued and exotic material was introduced  
631 from outside the caldera by sedimentary processes. Possible resurgent doming events  
632 contributed to these processes and influenced deposition of later pyroclastic density  
633 currents.



634 The Arran Volcanic Formation shows that a relatively small caldera can be active  
635 through a large number of eruptive periods, separated by significant time gaps, yet can  
636 escape large-scale intra-caldera faulting and formation of nested caldera structures,  
637 while accommodating significant, but not catastrophic, collapse. We argue that further  
638 detailed field investigation of similar calderas (including previously mapped examples),  
639 using modern physical volcanology methods and terminology, is essential to elucidate  
640 observations from active calderas and modelling experiments.

641

## 642 **Acknowledgements**

643 This study was undertaken as part of R. Gooday's PhD at Cardiff University, and was funded by  
644 NERC Studentship NE/L002434/1, as part of the Great Western 4+ Doctoral Training  
645 Partnership. The authors thank I. McDonald for undertaking geochemical analysis and A.  
646 Oldroyd for making excellent thin sections. We sincerely thank J. Fierstein, A Harris, V. Troll and  
647 an anonymous reviewer for their time and for greatly improving the manuscript.

648

## 649 **References**

- 650 Acocella, V. (2007). Understanding caldera structure and development: An overview of analogue models  
651 compared to natural calderas. *Earth-Science Reviews*, 85(3-4), 125-160.
- 652 Acocella, V., Di Lorenzo, R., Newhall, C., and Scandone, R. (2015). An overview of recent (1988 to 2014)  
653 caldera unrest: Knowledge and perspectives. *Reviews of Geophysics*, 53(3):896-955.
- 654 Almond, D. C. (1971). Ignimbrite vents in the Sabaloka cauldron, Sudan. *Geological Magazine*, 108(2),  
655 159-176.
- 656 Andrews, G. D. and Branney, M. J. (2011). Emplacement and rheomorphic deformation of a large, lava-  
657 like rhyolitic ignimbrite: Grey's Landing, southern Idaho. *Geological Society of America Bulletin*, 123(3-

- 658 4):725–743.
- 659 Bailey, E. B., Clough, C. T., Wright, W. B., Richey, J. E., and Wilson, G. V. (1924). Tertiary and Post-Tertiary  
660 Geology of Mull, Loch Aline, and Oban: A Description of Parts of Sheets 43, 44, 51, and 52 of the  
661 Geological Map, volume 43. HM Stationery Office.
- 662 Bell, B. R., & Emeleus, C. H. (1988). A review of silicic pyroclastic rocks of the British Tertiary Volcanic  
663 Province. Geological Society, London, Special Publications, 39(1):365-379.
- 664 BGS (1987). Arran, Scotland Special Sheet; 1:50 000 Series; Third Solid Edition. British Geological Survey.
- 665 Branney, M. J. and Kokelaar, B. P. (2002). Pyroclastic density currents and the sedimentation of  
666 ignimbrites: Geological Society Memoir no. 27. The Geological Society, London.
- 667 Branney, M. J., Kokelaar, B. P., and McConnell, B. J. (1992). The Bad Step Tuff: a lava-like rheomorphic  
668 ignimbrite in a calkalkaline piecemeal caldera, English Lake District. *Bulletin of Volcanology*, 54(3):187–  
669 199.
- 670 Branney, M. J., Bonnicksen, B., Andrews, G. D. M., Ellis, B., Barry, T. L., and McCurry, M. (2008). ‘Snake  
671 River (SR)-type’volcanism at the Yellowstone hotspot track: distinctive products from unusual, high-  
672 temperature silicic super-eruptions. *Bulletin of Volcanology*, 70(3):293-314.
- 673 Brown, R. J., and Branney, M. J. (2013). Internal flow variations and diachronous sedimentation within  
674 extensive, sustained, density-stratified pyroclastic density currents flowing down gentle slopes, as  
675 revealed by the internal architectures of ignimbrites on Tenerife. *Bulletin of volcanology*, 75(7):727.
- 676 Brown, R. J., Kokelaar, B. P., and Branney, M. J. (2007). Widespread transport of pyroclastic density  
677 currents from a large silicic tuff ring: the Glaramara tuff, Scafell caldera, English Lake District, UK.  
678 *Sedimentology*, 54(5):1163-1190.
- 679 Brown, R. J., Orsi, G., and de Vita, S. (2008). New insights into Late Pleistocene explosive volcanic activity  
680 and caldera formation on Ischia (southern Italy). *Bulletin of Volcanology*, 70(5):583-603.
- 681 Brown, D. J. and Bell, B. R. (2013). The emplacement of a large, chemically zoned, rheomorphic, lava-like  
682 ignimbrite: the Sgurr of Eigg Pitchstone, NW Scotland. *Journal of the Geological Society*, 170(5):753–767.

683 Brown, D. J., Holohan, E. P., and Bell, B. R. (2009). Sedimentary and volcano-tectonic processes in the  
684 British Paleocene Igneous Province: a review. *Geological Magazine*, 146(03):326– 352.

685 Cashman, K. V., and Giordano, G. (2014). Calderas and magma reservoirs. *Journal of Volcanology and*  
686 *Geothermal Research*, 288:28-45.

687 Chambers, L. M. (2000). Age and duration of the British Tertiary Igneous Province: implications for the  
688 development of the ancestral Iceland plume. PhD thesis, University of Edinburgh.

689 Cole, J. W., Milner, D. M., and Spinks, K. D. (2005). Calderas and caldera structures: a review. *Earth-*  
690 *Science Reviews*, 69(1-2):1-26.

691 Di Giuseppe, M. G., Troiano, A., and Carlino, S. (2017). Magnetotelluric imaging of the resurgent caldera  
692 on the island of Ischia (southern Italy): inferences for its structure and activity. *Bulletin of Volcanology*,  
693 79(12):85.

694 Druitt, T. H., and Sparks, R. S. J. (1984). On the formation of calderas during ignimbrite eruptions.  
695 *Nature*, 310(5979):679.

696 Emeleus, C. H. and Bell, B. R. (2005). The Palaeogene volcanic districts of Scotland, volume 3. British  
697 Geological Survey.

698 Geshi, N., Acocella, V., and Ruch, J. (2012). From structure- to erosion-controlled subsiding calderas:  
699 evidence thresholds and mechanics. *Bulletin of volcanology*, 74(6):1553-1567.

700 Geshi, N., and Miyabuchi, Y. (2016). Conduit enlargement during the precursory Plinian eruption of Aira  
701 Caldera, Japan. *Bulletin of Volcanology*, 78(9):63.

702 Gregory, J. and Tyrell, G. (1924). Excursion to Arran: July 27th to August 3rd, 1923. *Proceedings of the*  
703 *Geologists' Association*, 35(4):401.

704 Gudmundsson, A. (1988). Formation of collapse calderas. *Geology*, 16(9):808-810.

705 Gudmundsson, A. (1998). Formation and development of normal-fault calderas and the initiation of  
706 large explosive eruptions. *Bulletin of Volcanology*, 60(3):160-170.

707 Gunn, W., Peach, B. N., and Newton, E. T. (1901). On a remarkable volcanic vent of Tertiary age in the

708 Island of Arran, enclosing Mesozoic fossiliferous rocks. *Quarterly Journal of the Geological Society*, 57(1-  
709 4):226–243.

710 Hartley, M. E., & Thordarson, T. (2012). Formation of Öskjuvatn caldera at Askja, North Iceland:  
711 Mechanism of caldera collapse and implications for the lateral flow hypothesis. *Journal of Volcanology*  
712 and *Geothermal Research*, 227, 85-101.

713 Hildreth, W., and Fierstein, J. (2012). The Novarupta-Katmai eruption of 1912: largest eruption of the  
714 twentieth century: centennial perspectives (No. 1791). Geological Survey (USGS).

715 Holohan, E., Troll, V. R., Errington, M., Donaldson, C., Nicoll, G., and Emeleus, C. (2009). The Southern  
716 Mountains Zone, Isle of Rum, Scotland: volcanic and sedimentary processes upon an uplifted and  
717 subsided magma chamber roof. *Geological Magazine*, 146(03):400–418.

718 Jordan, N. J., Rotolo, S. G., Williams, R., Speranza, F., McIntosh, W. C., Branney, M. J., and Scaillet, S.  
719 (2018). Explosive eruptive history of Pantelleria, Italy: Repeated caldera collapse and ignimbrite  
720 emplacement at a peralkaline volcano. *Journal of Volcanology and Geothermal Research*, 349:47-73.

721 Kent, R. W. and Fitton, J. G. (2000). Mantle sources and melting dynamics in the British Palaeogene  
722 Igneous Province. *Journal of Petrology*, 41(7):1023–1040.

723 King, B. C. (1955). The Ard Bheinn area of the central igneous complex of Arran. *Quarterly Journal of the*  
724 *Geological Society*, 110(1-4):323–355.

725 King, B. C. (1959). Age of the granites of the Ard Bheinn area, Arran. *Proceedings of the Geological*  
726 *Society of London*, 1569:134.

727 Knott, T. R., Reichow, M. K., Branney, M. J., Finn, D. R., Coe, R. S., Storey, M., and Bonnicksen, B. (2016).  
728 Rheomorphic ignimbrites of the Rogerson Formation, central Snake River plain, USA: record of mid-  
729 Miocene rhyolitic explosive eruptions and associated crustal subsidence along the Yellowstone hotspot  
730 track. *Bulletin of Volcanology*, 78(4), 23.

731 Lavallée, Y., de Silva, S. L., Salas, G., and Byrnes, J. M. (2006). Explosive volcanism (VEI 6) without caldera  
732 formation: insight from Huaynaputina volcano, southern Peru. *Bulletin of Volcanology*, 68:333–348

733 Lipman, P. W. (1976). Caldera-collapse breccias in the western San Juan Mountains,

- 734 Colorado. Geological Society of America Bulletin, 87(10), 1397-1410.
- 735 Lipman, P. W. (1997). Subsidence of ash-flow calderas: relation to caldera size and magma-chamber  
736 geometry. Bulletin of volcanology, 59(3), 198-218.
- 737 Luchetti, A. C. F., Nardy, A. J. R., and Madeira, J. (2017). Silicic, high- to extremely high-grade ignimbrites  
738 and associated deposits from the Paraná Magmatic Province, southern Brazil. Journal of Volcanology  
739 and Geothermal Research
- 740 McDonald, I. and Viljoen, K. (2006). Platinum-group element geochemistry of mantle eclogites: a  
741 reconnaissance study of xenoliths from the Orapa kimberlite, Botswana. Applied Earth Science,  
742 115(3):81–93.
- 743 Meade, F. C., Chew, D. M., Troll, V. R., Ellam, R. M., and Page, L. (2009). Magma Ascent along a major  
744 terrane boundary: crustal contamination and Magma mixing at the Drumadoon Intrusive complex, Isle  
745 of Arran, Scotland. Journal of Petrology, 50(12):2345–2374.
- 746 Mellors, R. and Sparks, R. (1991). Spatter-rich pyroclastic flow deposits on Santorini, Greece. Bulletin of  
747 Volcanology, 53(5):327–342.
- 748 Moore, I. and Kokelaar, P. (1998). Tectonically controlled piecemeal caldera collapse: A case study of  
749 Glencoe volcano, Scotland. Geological Society of America Bulletin, 110(11):1448– 1466.
- 750 Mori, J., and McKee, C. (1987). Outward-dipping ring-fault structure at Rabaul caldera as shown by  
751 earthquake locations. Science, 235(4785):193-195.
- 752 Newhall, C. G., and Dzurisin, D. (1988). Historical unrest at the large calderas of the world (Vol. 2, No.  
753 1855). Department of the Interior, US Geological Survey.
- 754 Nobile, A., Acocella, V., Ruch, J., Aoki, Y., Borgstrom, S., Siniscalchi, V., and Geshi, N. (2017). Steady  
755 subsidence of a repeatedly erupting caldera through InSAR observations: Aso, Japan. Bulletin of  
756 Volcanology, 79(5):32.
- 757 Saunders, A., Fitton, J., Kerr, A., Norry, M., and Kent, R. (1997). The North Atlantic Igneous Province.  
758 Large igneous provinces: Continental, oceanic, and planetary flood volcanism, 45–93.

- 759 Saunders, S. J. (2001). The shallow plumbing system of Rabaul caldera: a partially intruded ring fault?  
760 *Bulletin of volcanology*, 63(6):406-420.
- 761 Self, S., and Rampino, M. R. (1981). The 1883 eruption of Krakatau. *Nature*, 294(5843):699.
- 762 Self, S., Rampino, M. R., Newton, M. S., and Wolff, J. A. (1984). Volcanological study of the great  
763 Tambora eruption of 1815. *Geology*, 12(11):659-663.
- 764 Smith, N. J., and Kokelaar, B. P. (2013). Proximal record of the 273 ka Poris caldera-forming eruption, Las  
765 Cañadas, Tenerife. *Bulletin of Volcanology*, 75(11), 768.
- 766 Stephenson, D., Mendum, J. R., Fettes, D. J., and Leslie, A. G. (2013). The Dalradian rocks of Scotland: an  
767 introduction. *Proceedings of the Geologists' Association*, 124(1):3–82.
- 768 Stevenson, C. and Grove, C. (2014). Laccolithic Emplacement of the Northern Arran Granite, Scotland,  
769 Based on Magnetic Fabric Data. In Nemeth, K., editor, *Advances in Volcanology*. Springer.
- 770 Storey, M., Duncan, R. A., and Tegner, C. (2007). Timing and duration of volcanism in the North Atlantic  
771 Igneous Province: Implications for geodynamics and links to the Iceland hotspot. *Chemical Geology*,  
772 241(3):264–281.
- 773 Sumner, J. M. and Branney, M. J. (2002) The emplacement history of a remarkable heterogeneous,  
774 chemically zoned, rheomorphic and locally lava-like ignimbrite: 'TL' on Gran Canaria. *Journal of*  
775 *Volcanology and Geothermal Research*, 115(1–2):109-138
- 776 Thompson, R. and Gibson, S. A. (1991). Subcontinental mantle plumes, hotspots and pre-existing  
777 thinspots. *Journal of the Geological Society*, 148(6):973–977.
- 778 Trippanera, D., Ruch, J., Acocella, V., Thordarson, T., & Urbani, S. (2018). Interaction between central  
779 volcanoes and regional tectonics along divergent plate boundaries: Askja, Iceland. *Bulletin of*  
780 *Volcanology*, 80(1), 1.
- 781 Troll, V. R., Emeleus, C. H., and Donaldson, C. H. (2000). Caldera formation in the Rum central igneous  
782 complex, Scotland. *Bulletin of Volcanology*, 62(4-5):301–317.
- 783 Troll, V. R., Walter, T. R., and Schmincke, H.-U. (2002). Cyclic caldera collapse: Piston or piecemeal

784 subsidence? Field and experimental evidence. *Geology*, 30(2):135–138

785 Tyrell, G. W. (1928). *The geology of Arran*. Printed under the authority of HM Stationery Office.

786 Young, G. and Caldwell, W. (2012). The Northeast Arran Trough, the Corrie conundrum and the Highland  
787 Boundary Fault in the Firth of Clyde, SW Scotland. *Geological Magazine*, 149(4):578.

788

789 **Fig. 1** Simplified geological map of the Isle of Arran, adapted from BGS (1987), with additional  
790 information from this study. The grid shows the 10 km eastings and northings of the British  
791 National Grid. Inset shows the onshore locations of magmatic rocks that make up the British  
792 Palaeogene Igneous Province in western Scotland and Northern Ireland. 1 – Skye, 2 – Rùm and  
793 Eigg, 3 – Ardnamurchan, 4 – Mull, 5 – Arran, 6 – Antrim, 7 – The Mourne Mountains, 8 – Slieve  
794 Gullion and Carlingford.

795 **Fig. 2** Geological map of the western half of the Central Arran Igneous Complex. Approximate  
796 locations of stratigraphic logs presented in this paper are shown in red. 1 – Ard Bheinn  
797 Member, 2 – Creag an Fheidh Member, 3 – White Tuff Member, 4 – Pigeon Cave Member, 5 –  
798 Ard Bheinn Member. The grid shows the 1 km eastings and northings of the British National  
799 Grid. Inset shows the location of the Central Arran Igneous Complex (CAIC) on Arran in relation  
800 to the North Arran Granite (NAG).

801 **Fig. 3** Overview of the hills Ard Bheinn and Binnein na h-Uaimh taken from the west. The  
802 coloured overlay shows the underlying geological units of the Arran Volcanic Formation. The  
803 uncoloured parts show areas underlain by the pre-caldera country rock. The summits of Ard  
804 Bheinn and Binnein na h-Uaimh are 670 m apart.

805 **Fig. 4** Generalised stratigraphic log of the Arran Volcanic Formation, showing the relationships  
806 between the pyroclastic and sedimentary units and major hiatus events. Vertical thicknesses  
807 are not to scale. Map symbols are consistent with those in Fig 3.

808 **Fig. 5** a) Stratigraphic log of the Muileann Gaoithe Member on the south side of Muileann  
809 Gaoithe. b) Folded flow-banding in the lower part of the unit, looking north west. c)  
810 Photomicrograph of the rhyolitic lava-like ignimbrite from the top of the Muileann Gaoithe  
811 Member. Viewed in plane-polarised light. Q – quartz, F – feldspar. The micro-scale flow fabric is  
812 defined by texturally/compositionally distinct (different colours) sub-mm and near-continuous  
813 bands and prolate rods. d) Photomicrograph of the rhyolitic lava-like ignimbrite from the base  
814 of the Muileann Gaoithe Member. Viewed in plane-polarised light. Q – quartz, F – feldspar. The  
815 flow fabric is defined by continuous bands.

816 **Fig. 6** a) Stratigraphic log of the Allt Ruadh Member along the Allt Ruadh section. b) A typical  
817 exposure of orange-weathering massive lapilli tuff (mLT) found in the Allt Ruadh Member. c)

818 Photomicrograph of typical mLT showing clasts of schist (left), dolerite (right), and altered  
819 rhyolite (bottom). Viewed in plane-polarised light. d) Photomicrograph of a glassy eutaxitic- to  
820 lava-like tuff containing crystals of quartz (Q), K-feldspar (F), and Fe-Ti oxides (ox). Viewed in  
821 plane-polarised light.

822 **Fig. 7** a) Stratigraphic log of the Creag an Fheidh Member along the Creag an Fheidh section. b)  
823 A massive lapilli tuff in the upper part of the unit. c) Photomicrograph of a massive lapilli tuff  
824 from the upper part of the member. Viewed in plane-polarised light. d) Photomicrograph of a  
825 eutaxitic tuff from the lower part of the unit, showing flattened clasts (fc) as well as quartz (Q),  
826 K-feldspar (F), and Fe-Ti oxide (ox) crystals. Viewed in plane-polarised light.

827 **Fig. 8** Finely laminated and cross laminated basaltic-andesitic tuff that makes up the Allt Beith  
828 tuff cone. Hammer for scale is 400 mm long.

829 **Fig. 9** a) Stratigraphic log of the White Tuff Member up the western slopes of Ard Bheinn. b)  
830 The thinly banded unit shown at around 415 m in the log. The meso-scale flow-fabric is clearly  
831 visible as bands of different colours, in this case yellow and grey. c) Photomicrograph of typical  
832 massive lava-like ignimbrite from the base of the member, showing the euhedral quartz crystals  
833 (Q) that are so characteristic of this ignimbrite, as well as K-feldspar (F) and Fe-Ti oxides (ox).  
834 Viewed in plane-polarised light. d) Photomicrograph of banded lava-like ignimbrite from the  
835 middle of the member, showing the flow fabric deformed around a large K-feldspar crystal (F).  
836 Viewed in plane-polarised light.

837 **Fig. 10** a) Stratigraphic log of the Pigeon Cave Member up the northern side of Binnein na h-  
838 Uaimh, where it is intruded by brecciated fingers of the basalt/dolerite sill. b) Stratigraphic log  
839 of the Pigeon Cave Member up the western side of Binnein na h-Uaimh, where it is not intruded  
840 by the sill. Dashed lines from a) show possible lateral bed correlations. c) Photograph showing a  
841 typical green-weathering massive lapilli agglomerate from the lower part of the Pigeon Cave  
842 Member. It contains elongate streaks and bands of rhyolitic material (rh). d) Photomicrograph  
843 of a crystal-rich lapilli tuff with a dark glassy groundmass, lithic lapilli (L), and quartz crystals (Q).  
844 Viewed in plane-polarised light. e) Photomicrograph of a crystal-rich agglomerate. The sickle-  
845 shaped wispy features are interpreted as small glassy cognate spatter clasts (sc). Viewed in  
846 plane-polarised light.

847 **Fig. 11** a) Stratigraphic log of the Ard Bheinn Member up the southern side of Ard Bheinn. b)  
848 Massive lapilli agglomerate near the summit on Binnein na h-Uaimh, looking north showing  
849 lithic lapilli (L) and elongate bands of rhyolite (rh). c) Photomicrograph of the feldspar (F) rich  
850 mTcr ('plagioclase porphyry' of King, 1955) from the summit of Ard Bheinn. Viewed between  
851 crossed polars. d) Eutaxitic massive lapilli tuff at 490 m elevation on the Ard Bheinn log,  
852 containing stretched out mafic clasts (mc). Pencil for scale is 150 mm long. e) Photomicrograph  
853 of the coarse crystal-rich tuff at the base of the Ard Bheinn Member, showing large quartz (Q)  
854 crystals and smaller K-feldspar crystals (F). Viewed in plane-polarised light.

855 **Fig. 12** A series of generalised cross sections through the Arran Volcanic Formation showing the  
856 history of eruption and caldera collapse. Lithologies other than the caldera-fill succession have

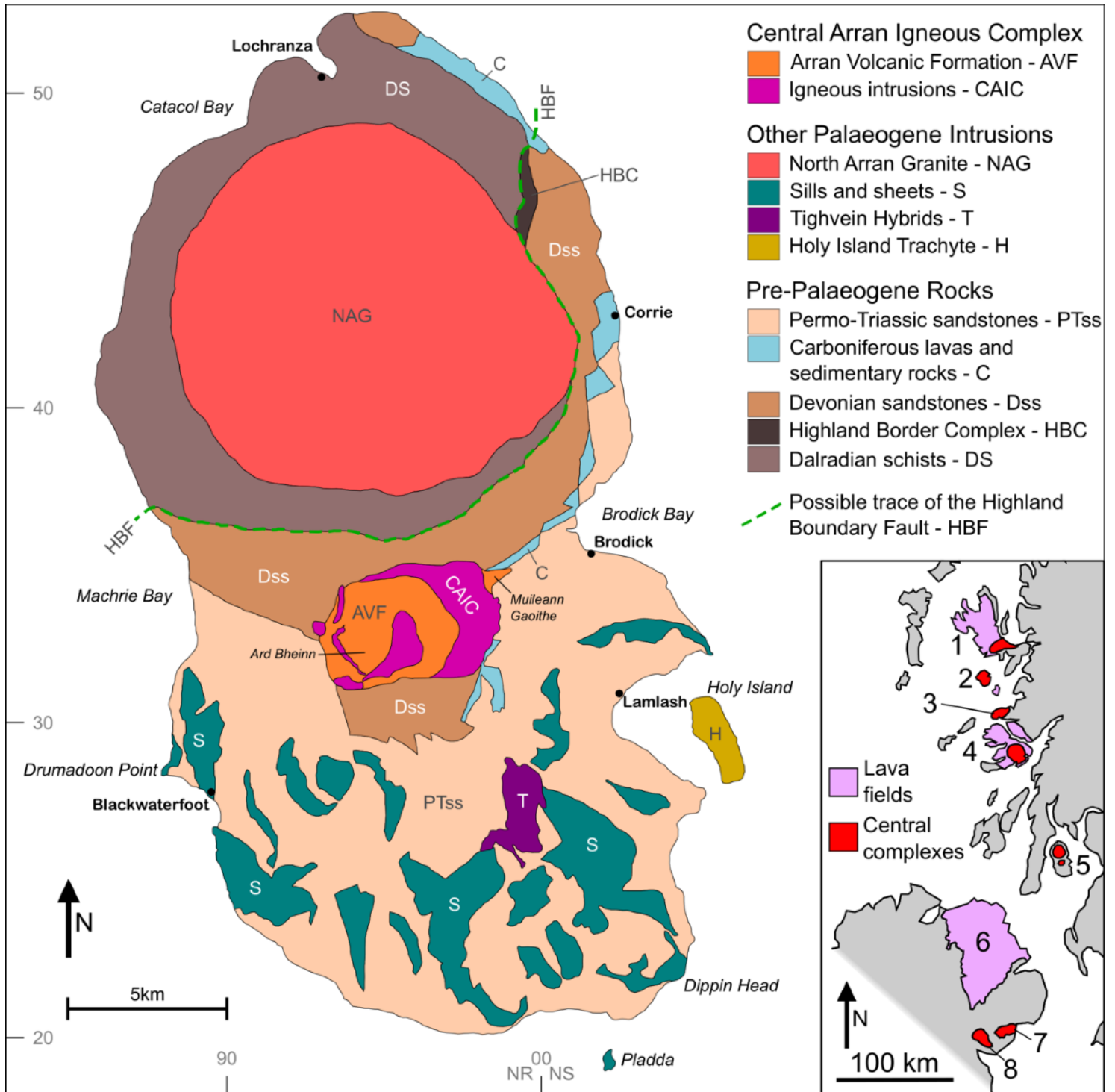


857 been omitted for clarity.

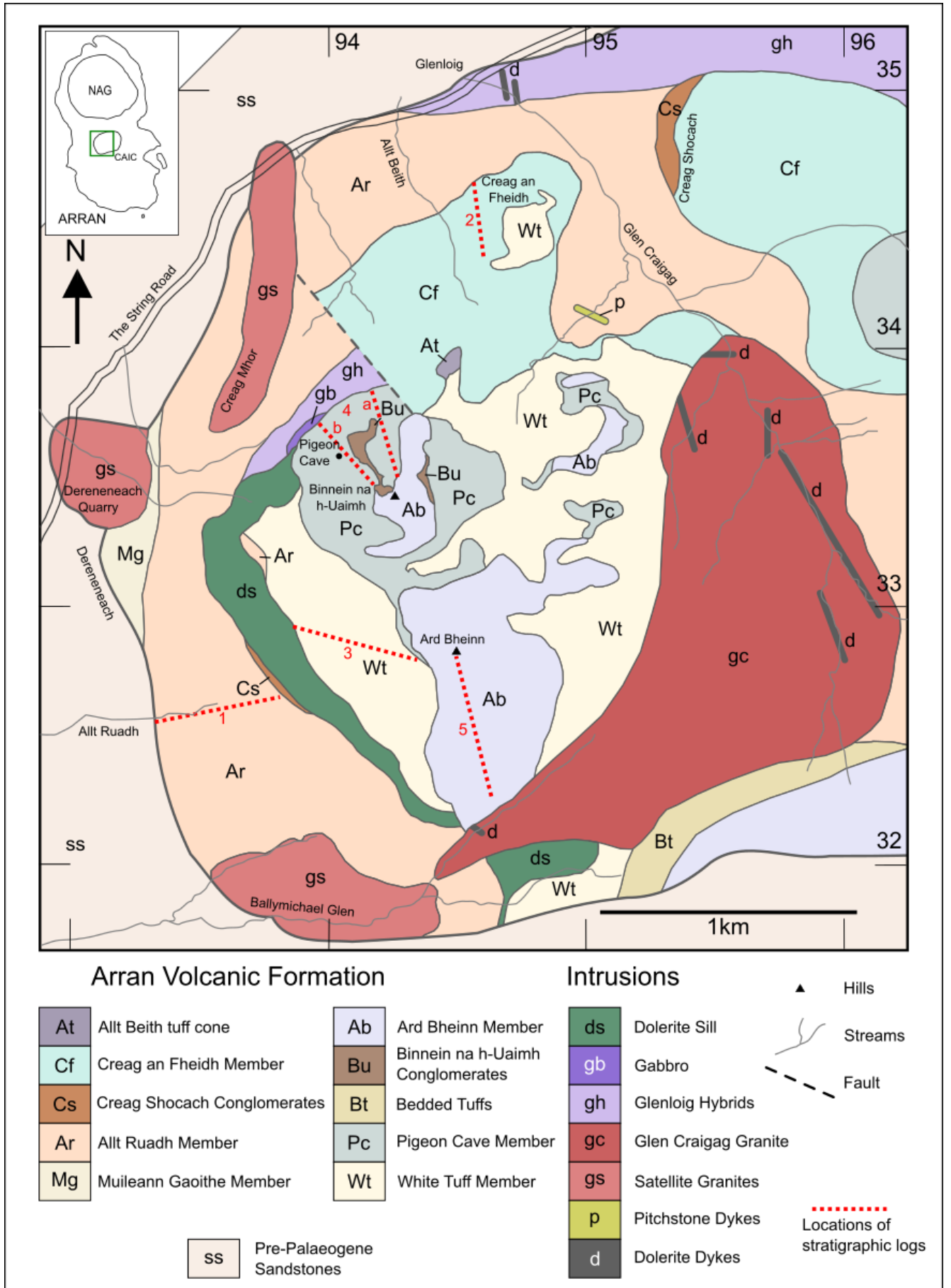
858 **Table 1** Descriptions and interpretations for the volcanic and sedimentary units that make up  
859 the Arran Volcanic Formation.

860 **Table 2** Explanation of ignimbrite lithofacies codes used in this paper, following the terminology  
861 of Branney and Kokelaar (2002).

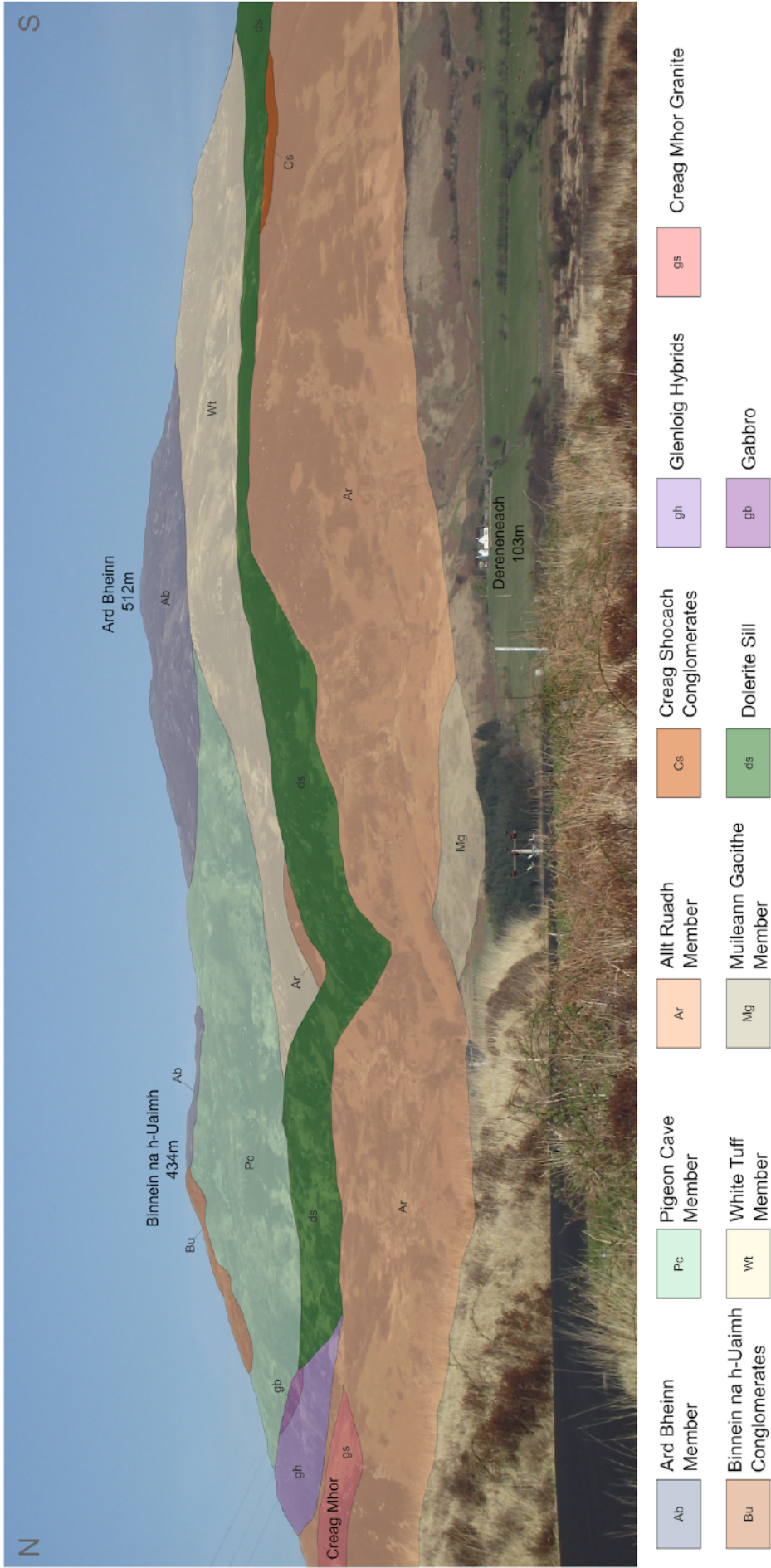
862 **Table 3** Anhydrous whole-rock geochemical data for various ignimbrite samples.



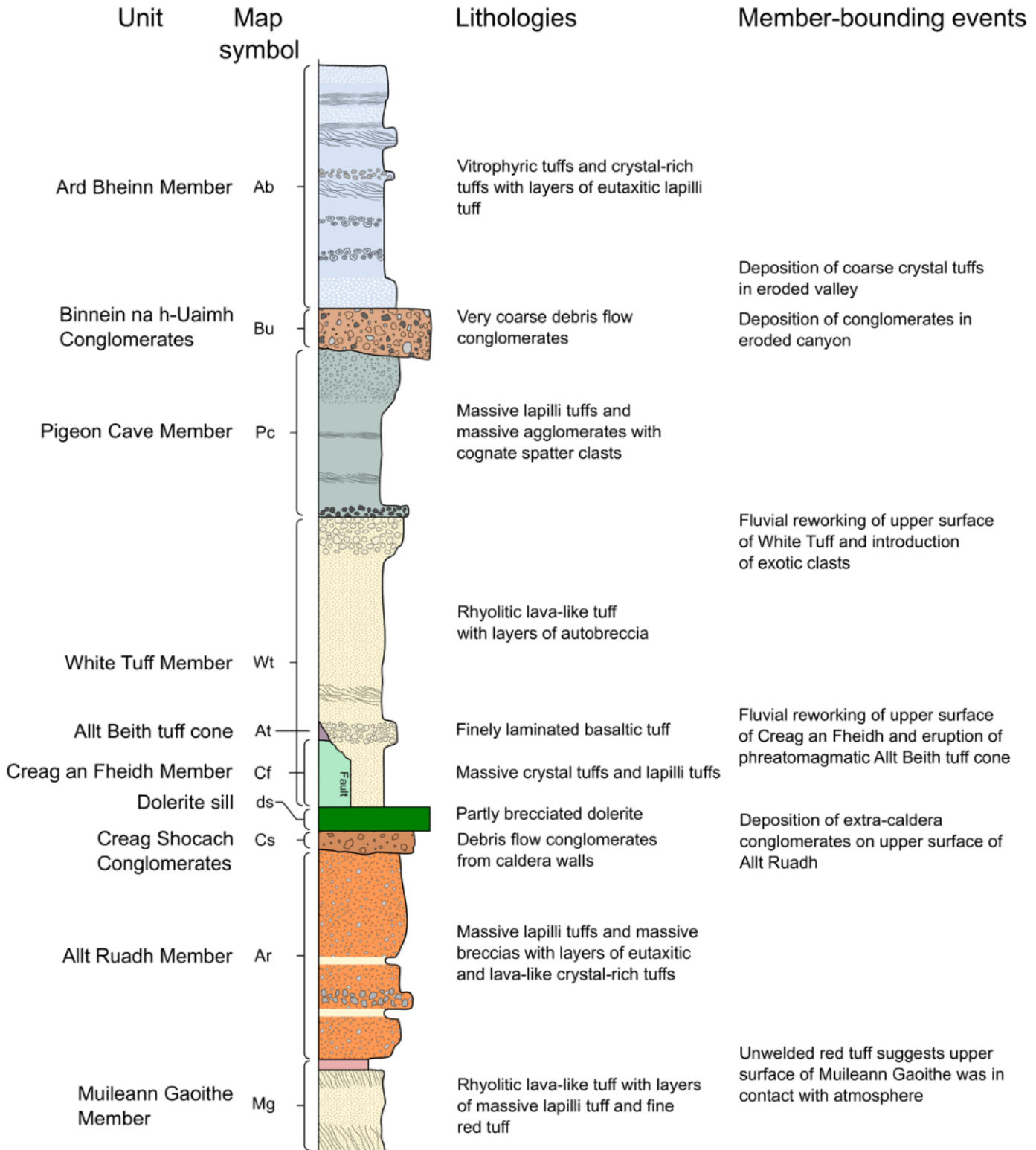
Figure



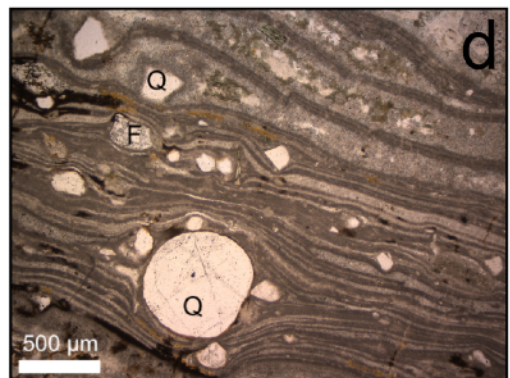
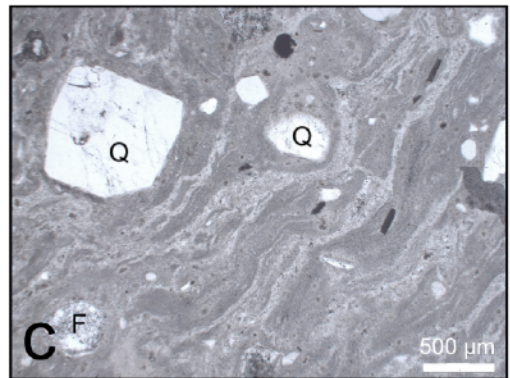
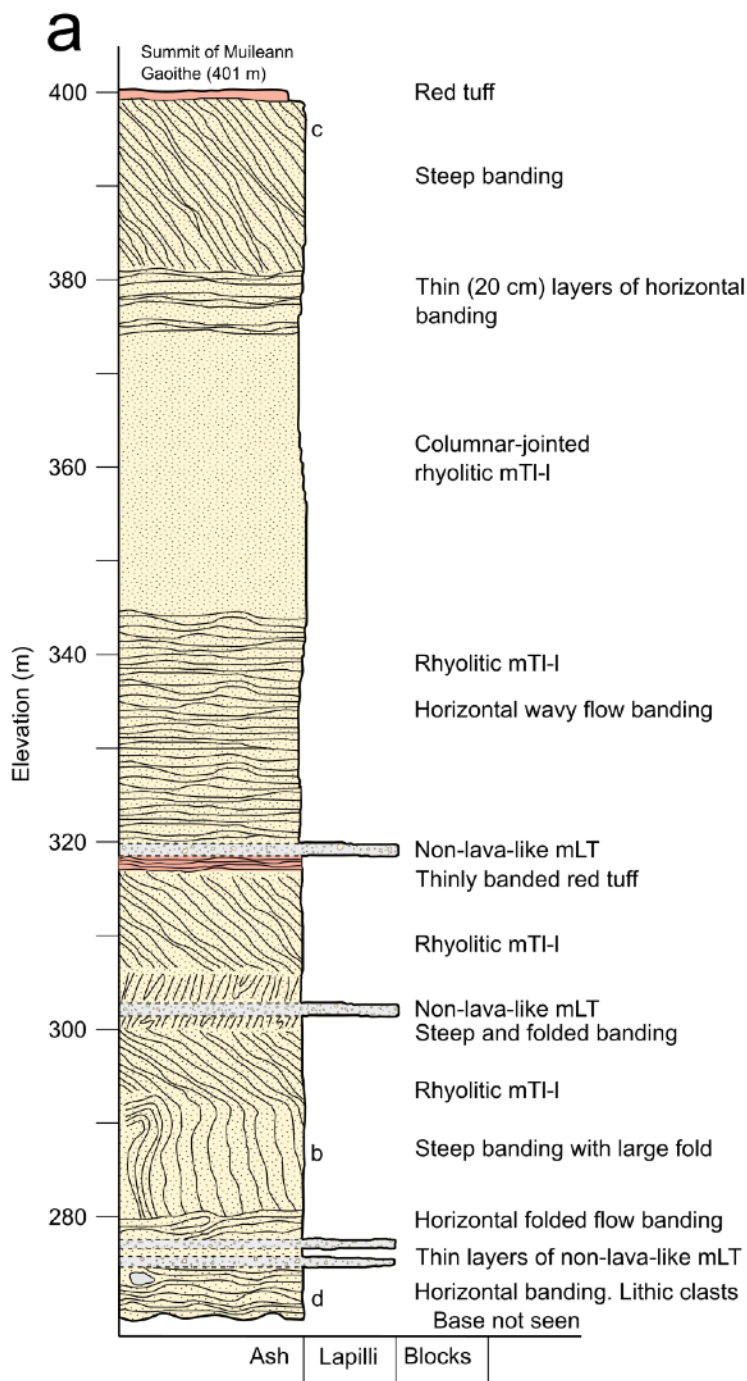
Figure



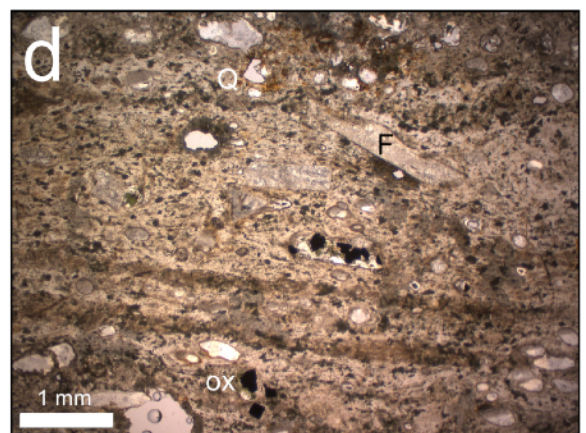
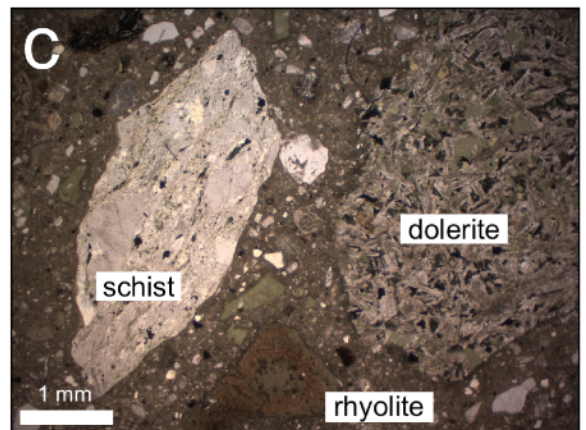
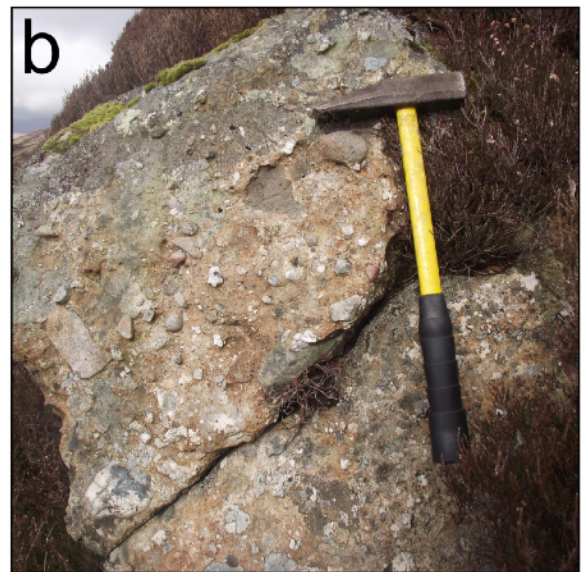
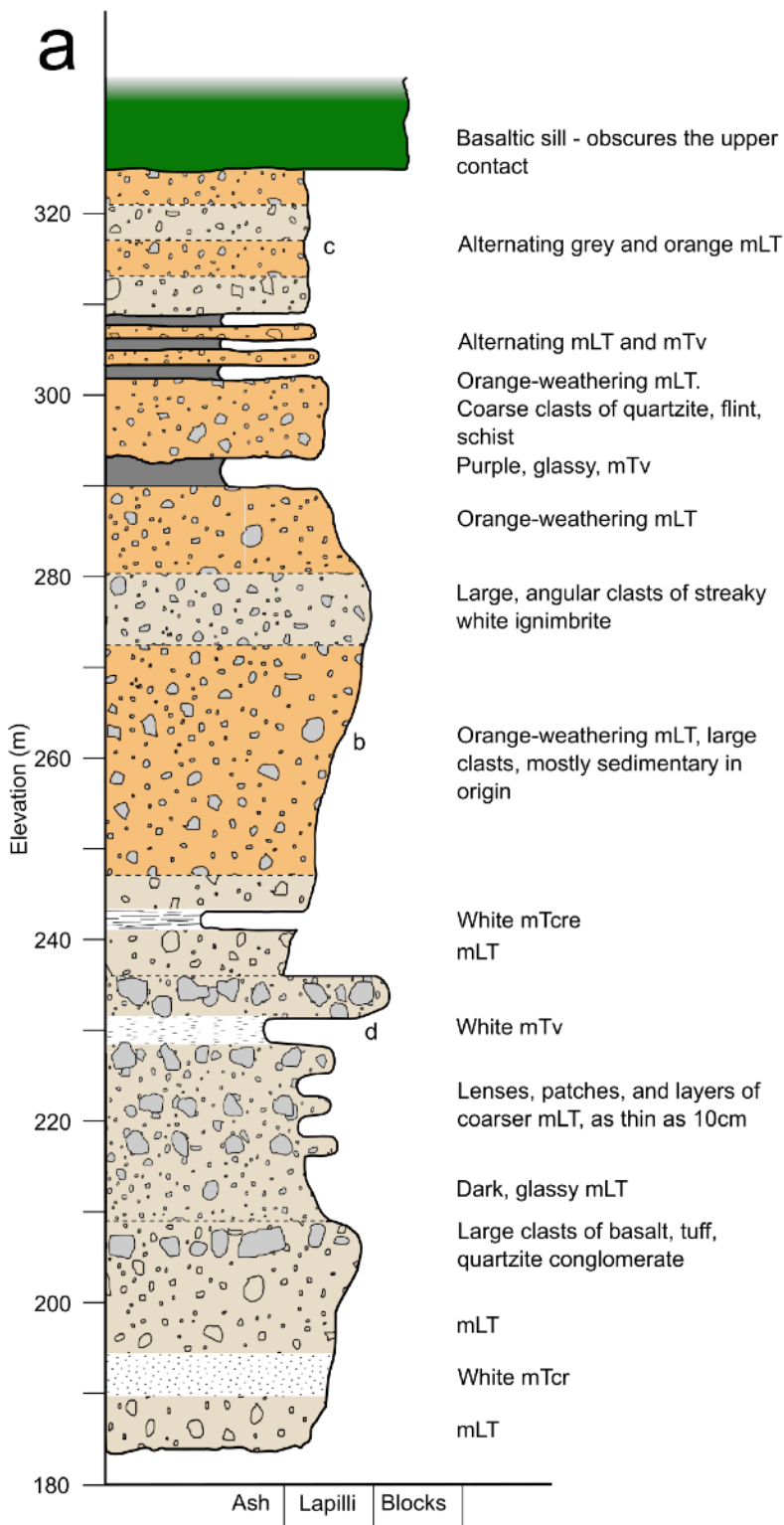
Figure



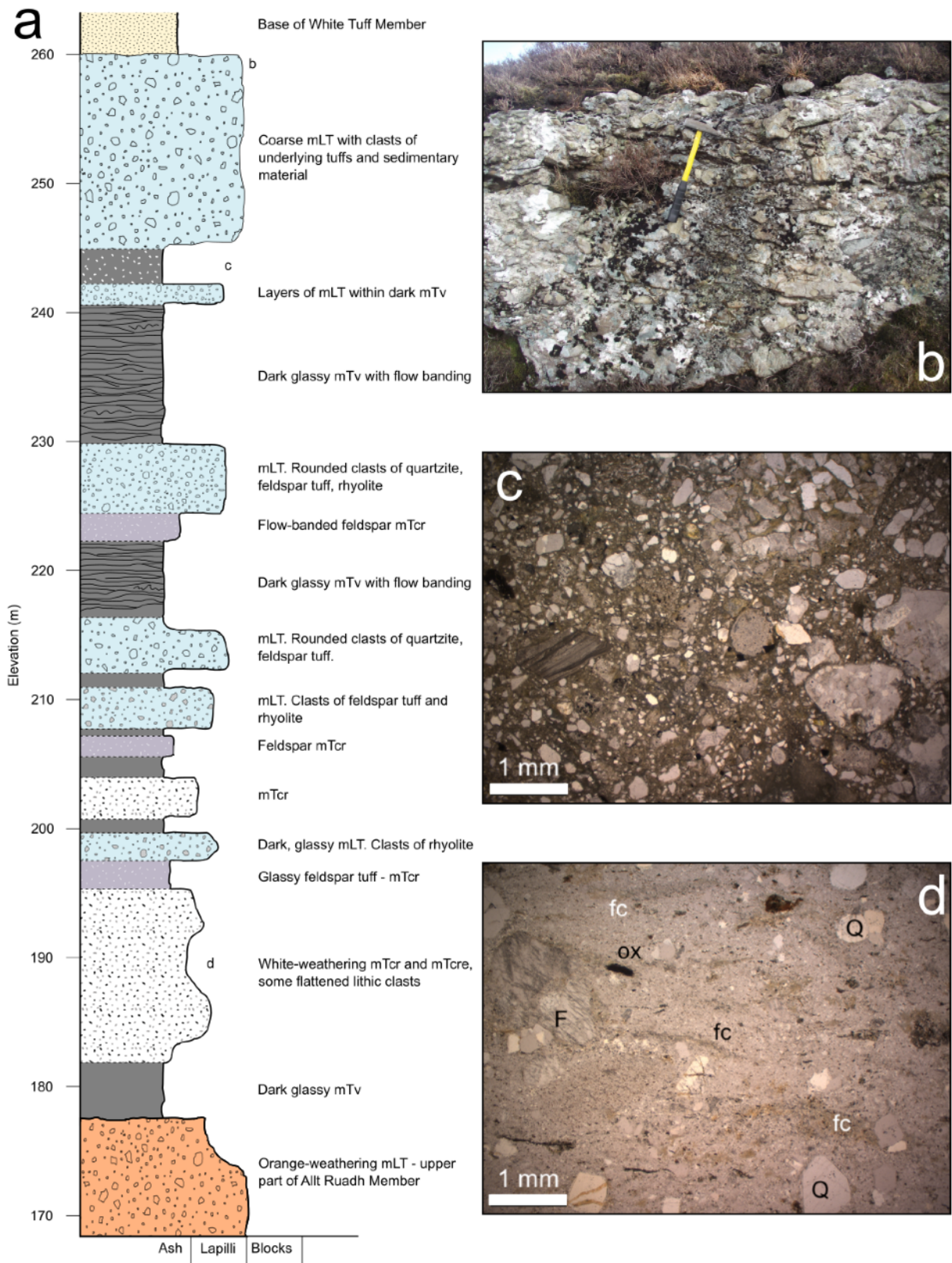
Figure



Figure



Figure

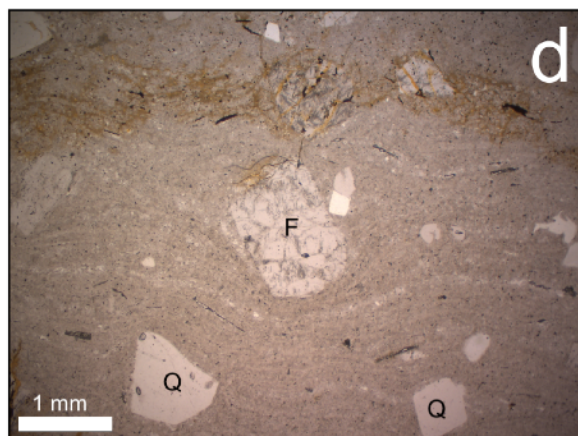
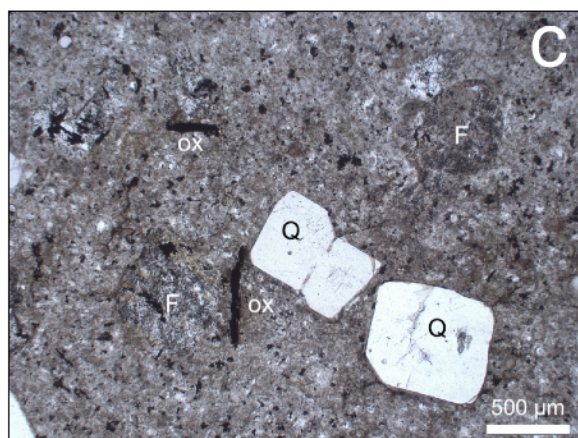
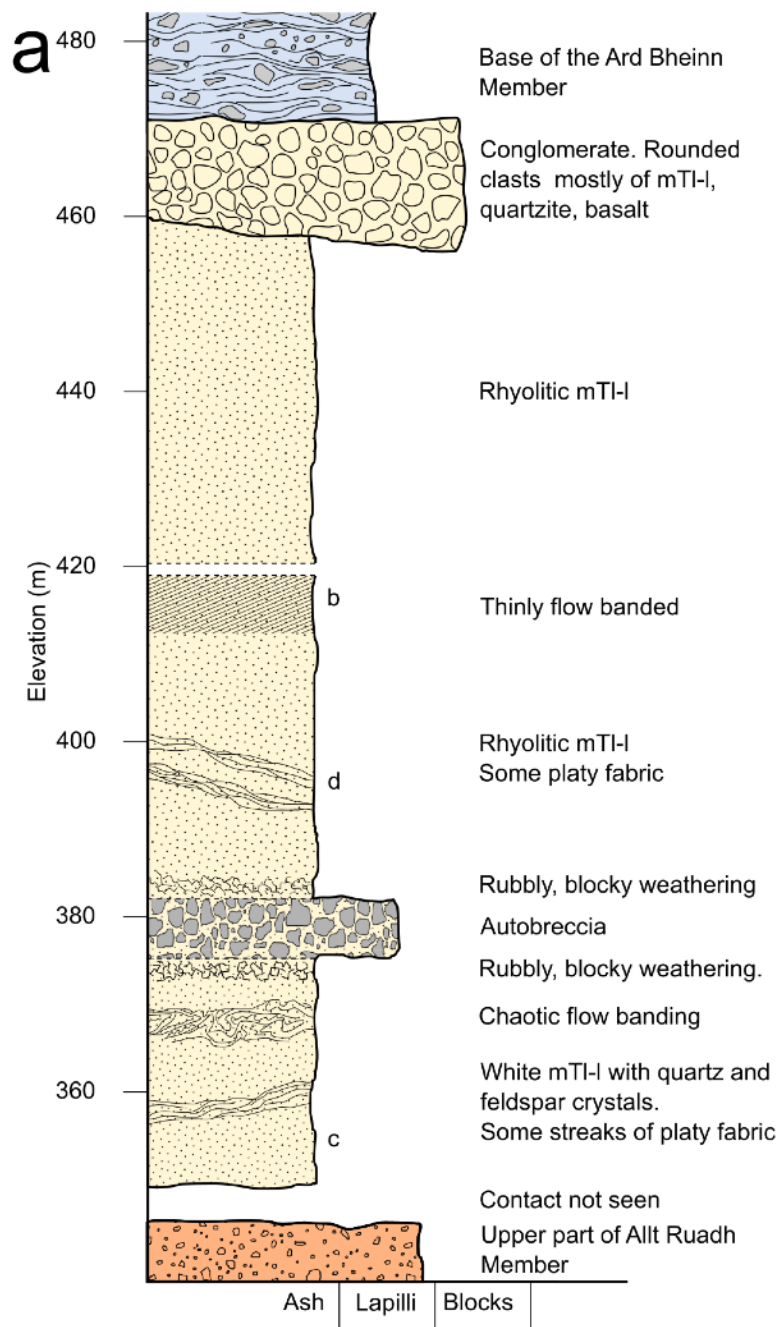


Figure

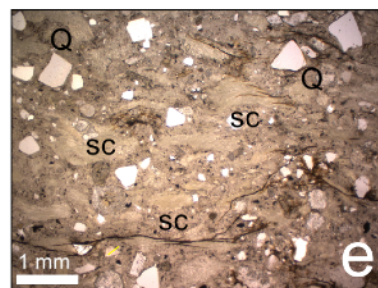
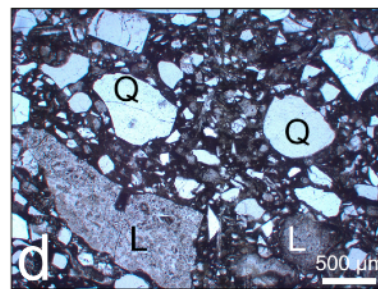
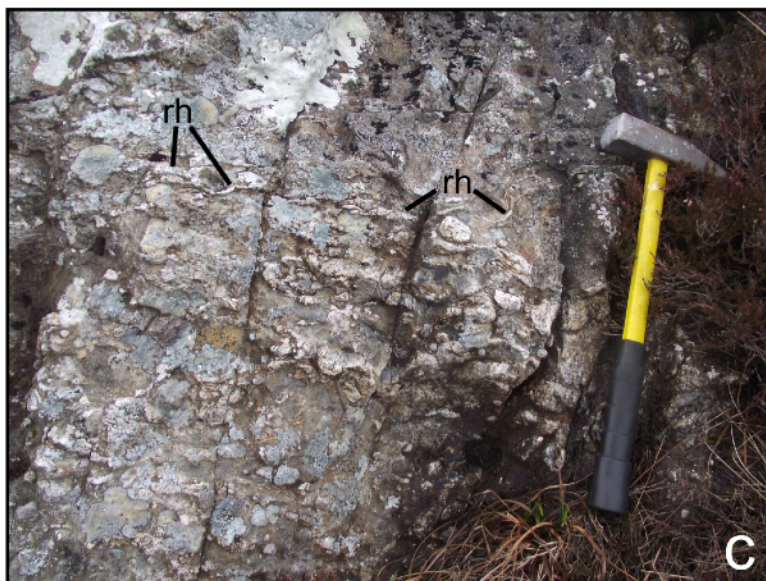
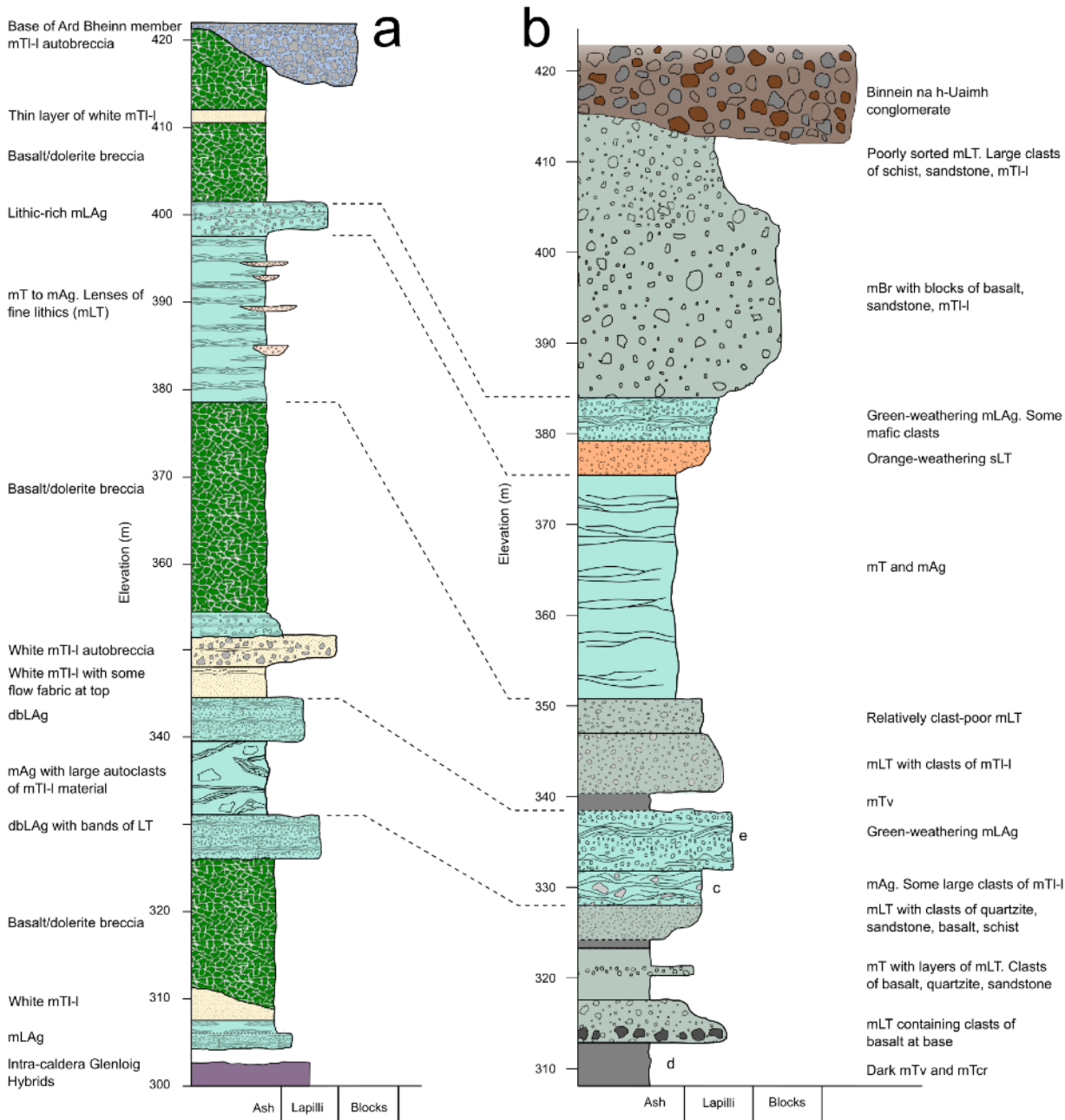




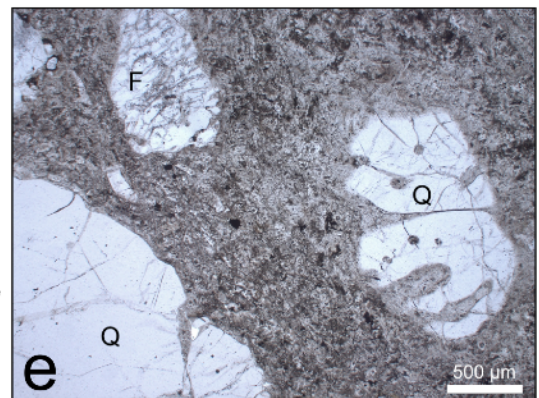
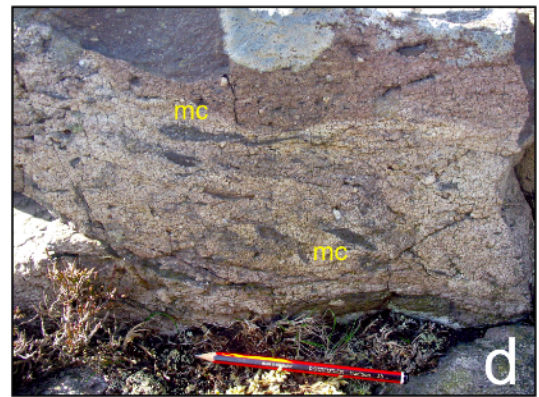
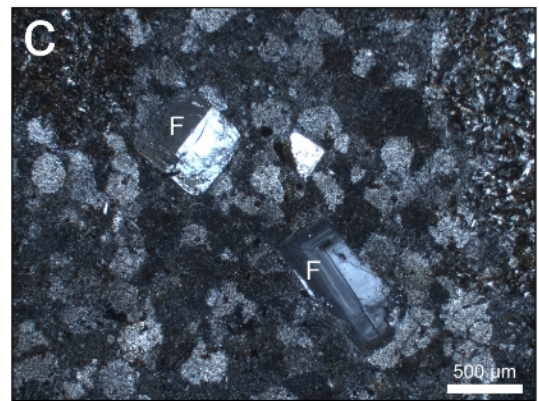
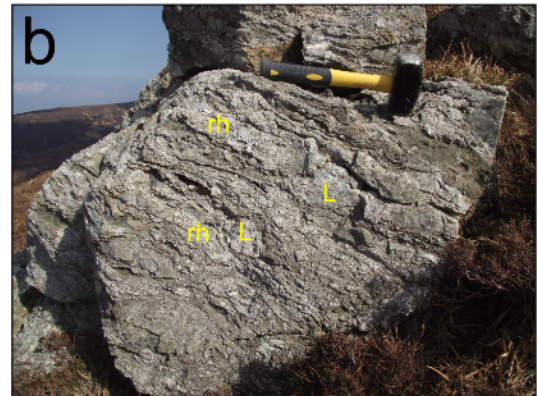
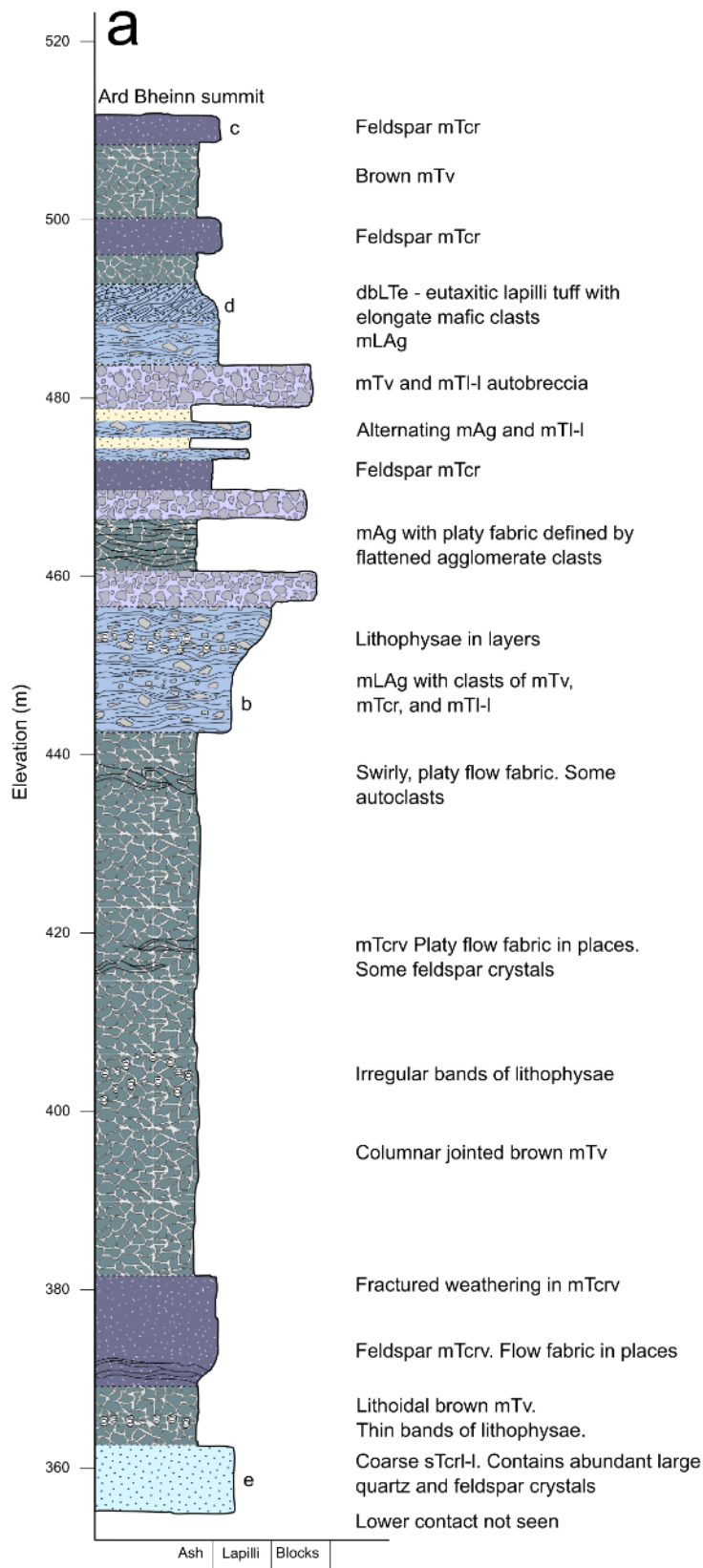
Figure



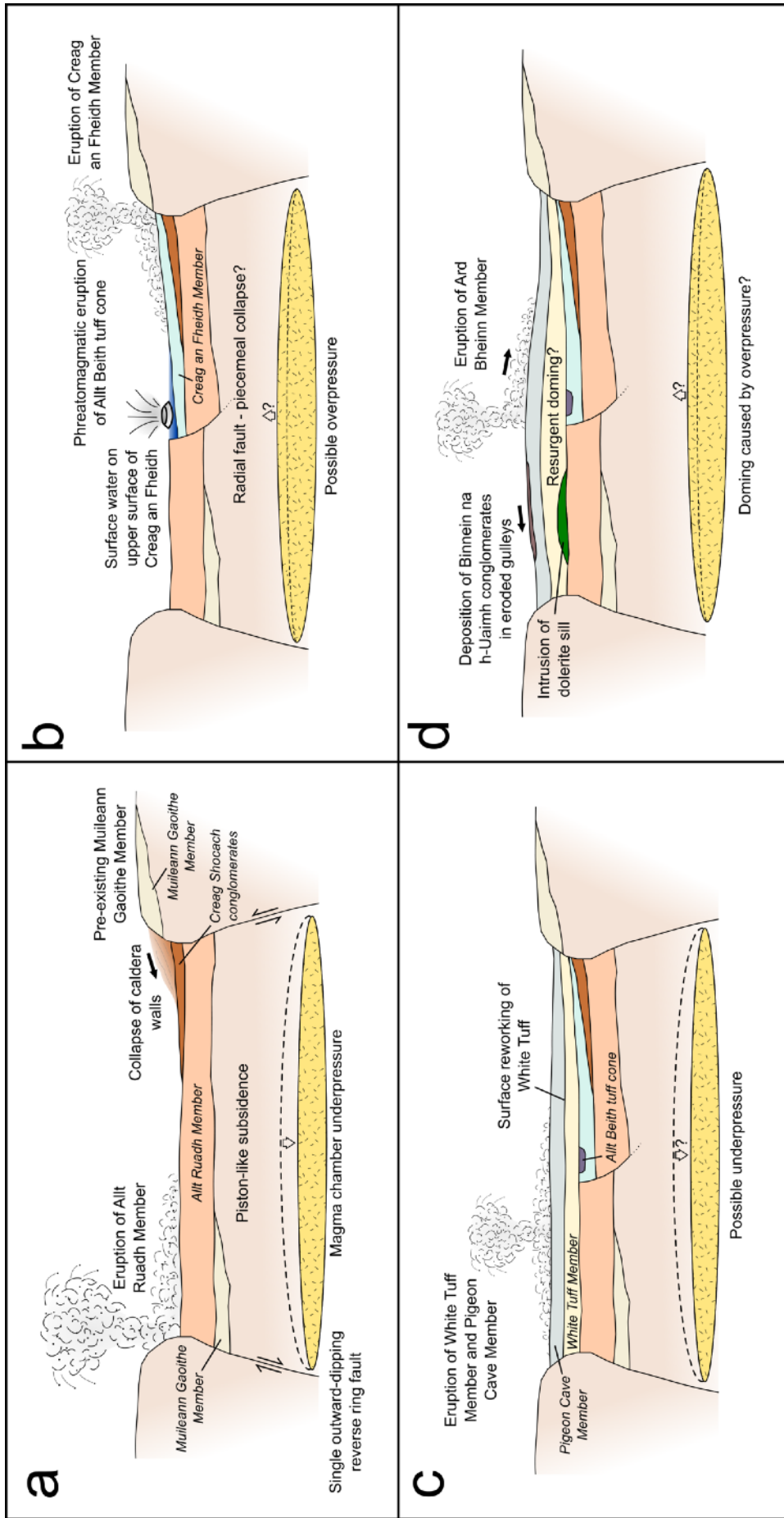
Figure



Figure



Figure



Figure